Development of an ATV-Based Remote-Operated Sensor Platform

Mark Sumner

Thesis submitted to the faculty of the
Virginia Polytechnic Institute and State University
in partial fulfillment of the requirements for the degree of

Masters
in
Mechanical Engineering

Martin Johnson, Chairman
James Carneal
Andrew Kurdila

April 30th, 2010
Blacksburg, VA

Keywords: Acoustic Localization, Sensor Platforms, Urban Combat, Sniper Detection, Remote-Operated Vehicles

Development of an ATV-Based Remote-Operated Sensor Platform

Mark Sumner

ABSTRACT

Urban warfare is unfortunate reality of the modern world and that fact is unlikely to change in the near future. One significant danger to soldiers in an urban setting is posed by concealed snipers. The large amount of cover among densely packed buildings make snipers hard to detect by sight or sound. When a sniper fires at troops, it is imperative to positively locate the sniper as soon as possible to ensure the safety of soldiers in the field.

One method of sniper detection is the use of distributed sensor nodes. These nodes may be stationary, mounted on a soldier or mounted on a vehicle. These nodes may accommodate many types of sensors, including microphones and cameras, both conventional and infrared. This project specifically deals with microphone arrays and conventional cameras mounted on a remote-operated vehicle. The purpose of this project is to demonstrate that mobile sensor platforms can be used alone or in groups to locate the source of gunshots as well as other sources of noise.

The vehicle described is a recreational ATV. It has been outfitted with mechanical actuators and electronic control modules to allow the vehicle to be operated remotely. The selection and installation of these components is detailed. This includes the control of the ATV's steering, brakes, throttle and engine starter. The system also includes a failsafe circuit to ensure that the system will shut down if positive control is lost.

An array of sensors and transducers was added to the vehicle to allow for useful data collection. This includes the aforementioned microphone array and camera. Other sensors mounted on the vehicle include a GPS antenna and an electronic compass for establishing the position and orientation of the vehicle and an accelerometer to sample engine vibration and allow for cancellation of engine noise.

Once assembled, this vehicle was tested in laboratory and field environments to demonstrate its effectiveness as a mobile sensor platform. The tests showed that a microphone array could be used in combination with a camera to provide a continuous stream of images of a moving target. The test also demonstrated how a mobile acoustic node can relocate to triangulate the location of an acoustic source and thereby replicate a larger stationary network. Overall, these tests demonstrated that such a system is a feasible platform for urban combat use. Full implementation would require the fusion of several separate features, the addition of a few new features, such as semi-autonomous operation, and further field testing.

Acknowledgements

I would like to first thank my advisor Dr. Marty Johnson for his support and instruction throughout my graduate career and for providing me with many challenging projects to work on. His guidance and insight made me a better student and engineer. I would like to further thank him for his incredible patience working with me remotely as I continued my research as a remote, part-time student with a full time job.

I would also like to thank Dr. Jamie Carneal for providing me with assistance and advice on my various projects. He was always happy to help with whatever problem arose in my research.

Thanks to Dr. Andy Kurdila for giving me the opportunity to interface with other members of the JOUSTER community and see other exciting applications of a similar sort to my main project. Without the funding and support of JOUSTER my project would not be possible.

Many thanks to Dr. Michael Roan for insight during weekly presentations and for his help getting parts of my mobile platform fabricated.

I would like to thank my fellow researchers, Dr. Philip Gillett and Dr. Dan Mennitt whose collaboration gave me the tools necessary to implement and test the various parts of my project. They were always available to bounce ideas off of to improve my designs. Their significant contribution of time and brain power will not go unappreciated.

I would be remiss without thanking Dr. Cory Papenfuss, who assisted me on many electrical problems, most notably the helping me to design the failsafe circuit that kept my mobile platform from going rogue. Thanks also to the other members of VAL who assisted me at various points in my project: Brent Gold, Elizabeth Hoppe, Caroline Hutchison, Ben Smith, and Tim Wiltgen.

A special thanks goes to our administrative assistant Gail Coe who kept our office running and kept everyone smiling, even if her candy jar kept a few extra pounds on me.

Finally I would like to extend my gratitude towards my wonderful my family for preparing me for collegiate life and sustaining me through the inevitable rough patches. Their constant love and encouragement ensured that I see this project through to fruition.

Table of Contents

List of Figures

Chapter 1: Introduction

1.1 Problem and Motivation

The purpose of this project is to explore the use of a mobile sensor platform as a standalone sensor array or a node in a larger network of sensor nodes. Such a platform would be a useful tool in an urban combat environment, particularly to detect the source of gunfire. Concealed sniper fire is one of the more pertinent dangers of urban combat. Urban environments are filled with obstructions and cover to hide the sniper from view as well as an abundance of interfering noise and many surfaces for sound to reflect from.

Thus JOUSTER (Joint Unmanned Systems Testing, Experimentation and Research) and VAL (Vibrations and Acoustics Laboratory), both of Virginia Tech, jointly undertook a project to field a team of sensor-equipped semi-autonomous vehicles as scouts in urban combat. The end goal of the project is for this fleet of vehicles to be able to collectively estimate the location of gunfire as well as other combat related noise sources (engines, tires, etc.) The fleet will also possess the ability to relocate to more favorable positions based upon the estimated locations of noise sources.

This project heavily utilized complementary work done by VAL members Philip Gillett and Daniel Mennitt. Gillett and Mennitt respectively focused on acoustic localization with a diffracting array [1] and target tracking with multiple arrays [2]. Gillett's work provided the calibrated acoustic array mounted on the ATV as well as the beamforming methods needed to convert raw acoustic data into useful bearing estimates. Mennitt's work proved the practical application of a mobile sensor node by demonstrating the methods by which an acoustic target could be tracked with one or more acoustic arrays. The collaboration of both resulted in software that could be used to keep track of the position of the mobile node while obtaining angle estimates of impulsive and tonal acoustic events.

Using a distributed network of acoustic sensor nodes to localize gunfire in an urban environment has been explored by many groups in recent years. G. Simon et al of Vanderbilt University describe a network of cheap sensors that would be more effective

than a centralized detection system [3]. There are a couple of reasons given for this hypothesis. First, such a network can tolerate the loss of a small number of nodes where a central sophisticated sensor cannot. Also, the distributed nature of the network allows for compensation of "multipath" effects, where the reflective surfaces of an urban environment propagate the sound of a gunshot along multiple paths.

S. Hengy of the French German Institute of Saint-Louis describes experiments using networks of helmet mounted acoustic arrays to detect gunshots as well as other battlefield events, such as vehicles passing nearby [4]. Each helmet array was able to estimate the angle of arrival of the gunshot. Hengy also describes ways of increasing the utility of the helmet mounted nodes by demonstrating how each node should be able to estimate the distance to the shooter as well as the caliber of weapon fired. S. Hengy et al later describe how such tests were successfully carried out in a realistic urban environment [5].

S. Young et al of the U. S. Army Research Laboratory performed work very similar to this project, using robot-mounted acoustic arrays to detect sniper fire in an urban setting [6], [7]. Their team incorporated several features that were attempted on this project. Young's system incorporates a cameras to look for the source of sound after an acoustic event has been detected as well as noise filtering to avoid detection of any noise generated by the robot itself. P. Martin follows up on Young's work and describes how information from such a network is collected and distilled to locate and tracker snipers and vehicles [8].

While this previous work focuses on using a network of sensor nodes to localize on a target, this project describes the implementation of a single mobile sensor node and demonstrates its effectiveness as a single node while showing how it can be used as part of a larger network.

1.2 Overview

The project consists of multiple phases: conversion of a standard recreational ATV to a remote-operated vehicle, instrumentation of the ATV with sensors and data

acquisition, testing individual system components and finally testing the effectiveness of the system as a mobile sensor node.

In order to convert the ATV to a remote-operated vehicle, it was necessary to first outfit the vehicle with actuators that could control the various functions of the ATV, specifically steering, braking, throttle control as well as starting and stopping the engine. Once mounted on the ATV, the actuators were connected to a control interface that allowed the vehicle to be operated remotely. This paper will discuss both the mechanical and electrical elements added to the ATV to allow for remote operation.

After remote conversion of the ATV, a sensor package was added to the vehicle to allow for useful data collection. This includes a GPS antenna and compass to determine the vehicle's location and orientation, a microphone array for sound detection, a video camera for transmitting useful visual data and an accelerometer to allow for engine noise cancellation. All of these elements are tied into an onboard computer which transmits selected data to a central server. This paper describes the selection, mounting and testing of the individual sensor components.

The paper then describes the testing of the complete system to demonstrate its usefulness as a mobile sensor node. This includes the integration of the camera with the acoustic node as well as a field test demonstrating triangulation of an acoustic source.

Chapter 2: ATV Remote Control Conversion

The first step in creating an autonomous sensor platform for this project is converting a gas-powered all-terrain vehicle (ATV) into a remotely controlled vehicle. This task is subdivided into mechanical and electrical conversion. Figure 2.1 shows the pre-conversion ATV with important features highlighted.

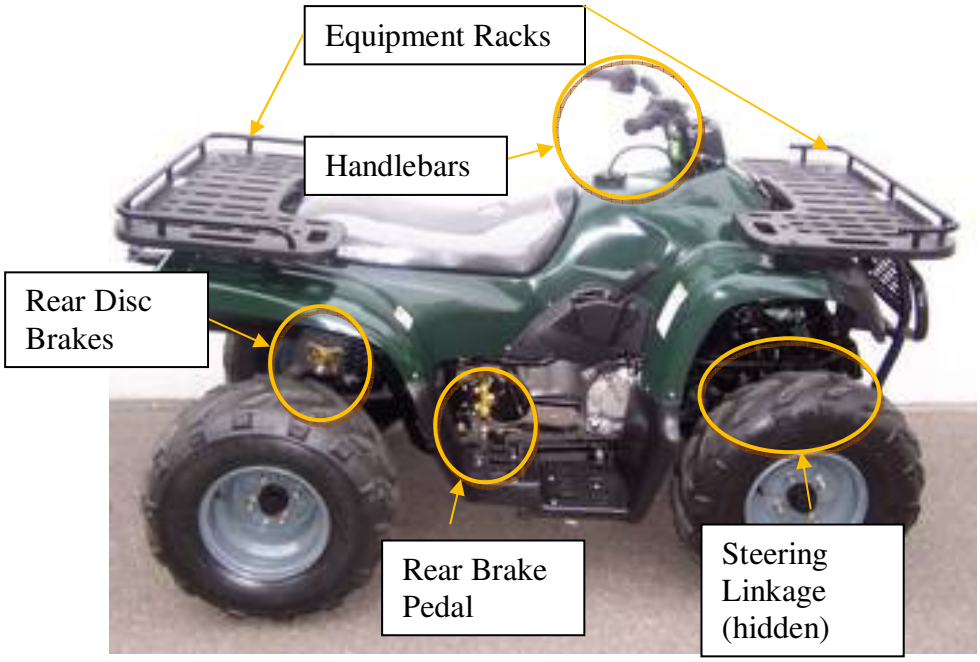

Figure 2.1: Diagram of the Kazuma Cougar 250 before conversion.

This chapter describes how the ATV was converted to a remotely controllable vehicle. The equipment used for this transition is detailed here as well as the methods used to install and setup this equipment. This chapter is divided into two subsections dealing with the mechanical and electrical components of the system conversion, respectively.

2.1 Mechanical Conversion

2.1.1 Steering System

The Kazuma Cougar 250 uses a standard ATV handlebar steering system with a dual A-arm suspension. The handlebars turn a steering column which in turn pushes and pulls tie rods. Each tie rod is attached by a ball and socket joint to the steering arms of the front wheels. The steering arms pivot with the wheel about the kingpin. Figure 2.2 shows a picture of the ATV steering and suspension system for the left front wheel.

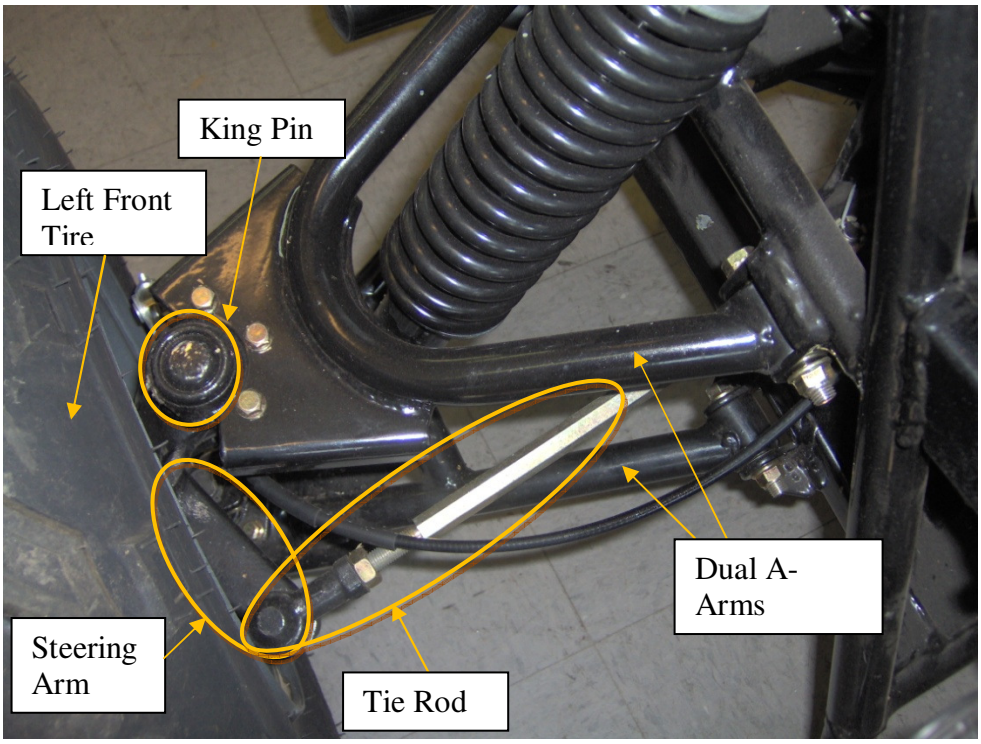

Figure 2.2: Picture of ATV front suspension.

Converting the steering of an ATV from manually-operated to remotely-operated requires attaching an actuator to some part of the steering system. The ATV conversion process began by formulating a basic design to perform this task. Multiple possibilities for attachment points as well as actuators were considered for the design.

Ultimately, the final design called for a linear actuator to push and pull the steering arm of the left wheel, similar to the tie rod. When selecting a linear actuator for

the application, the tie rod was used as a basis for comparison when considering the forces and range of travel required. The steering system requires 80 N*m of torque applied at the handle bars to move from either from fully left or fully right when the wheels are placed on a tile floor. With the steering arm measuring 15 cm long, a tie rod must exert approximately 530 N of force on the steering arm to turn one of the front wheels. The total range of motion for the steering system is approximately 60°, requiring a 15 cm range of travel for the tie rod, and similarly for the linear actuator.

With these criteria, the Ultramotion Bug [9] linear actuator was selected. The model chosen can produce up to 500 lbs (2200 N) of force and can produce the required 530 N at a 50% duty cycle. It also has an 8 inch (20 cm) stroke length.

In order to avoid interferences within the frame and suspension of the ATV, it became necessary to mount a plate to the steering arm to effectively lengthen it. With this steering arm extension, the attachment point for the linear actuator was moved out to 20 cm from the king pin. This extension also allowed the linear actuator to use all of its range of travel, eliminating the need for limit switches. With a moment arm of 20 cm, the required force output of the linear actuator becomes 400 N, which allows the linear actuator to operate close to the 100% duty cycle range.

The steering arm was extended by bolting an aluminum plate to the top of it. The linear actuator attaches to this extended arm with a quick-disconnect ball and socket joint. The base of the linear actuator is attached to the frame of the ATV with 2-axis pivoting assembly. The assembly allows for rotation about both the vertical axis and the lateral axis of the actuator. Rotation about the vertical axis is provided by a “Lazy Susan” bearing on which a square mounting bracket sits. Rotation about the lateral axis (rotation in the vertical plane) is enabled by a square mounting bracket through which shoulder bolts attach to the actuator’s trunion mount. This mounting system can be seen in Figure 2.3. Figure 2.4 shows the actuator arm attached to the extended steering arm.

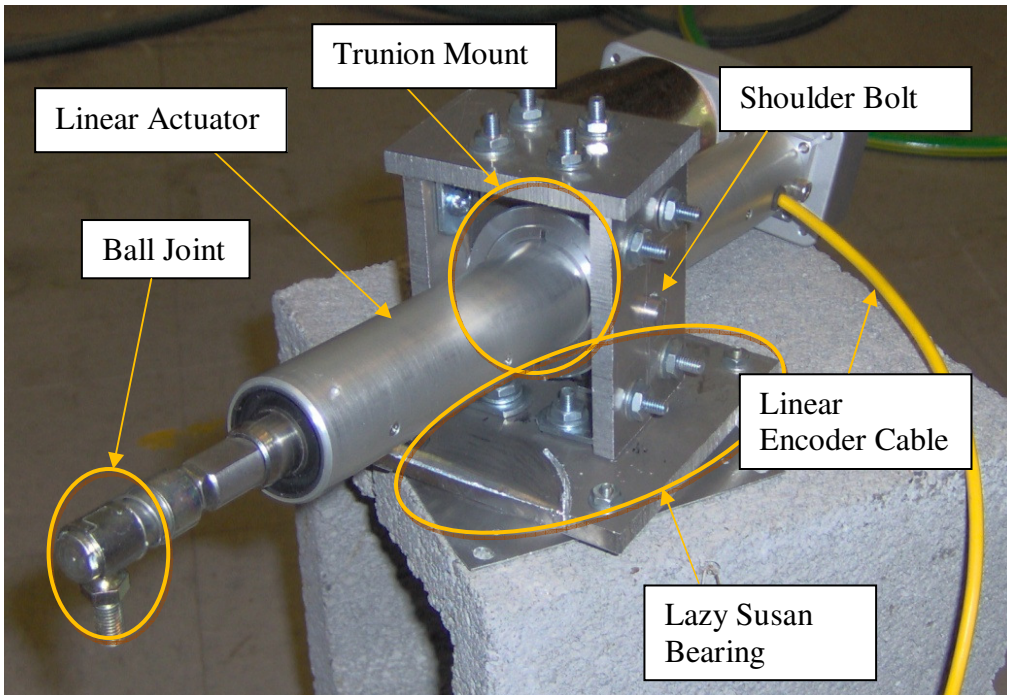

Figure 2.3: Steering linear actuator and mounting bracket.

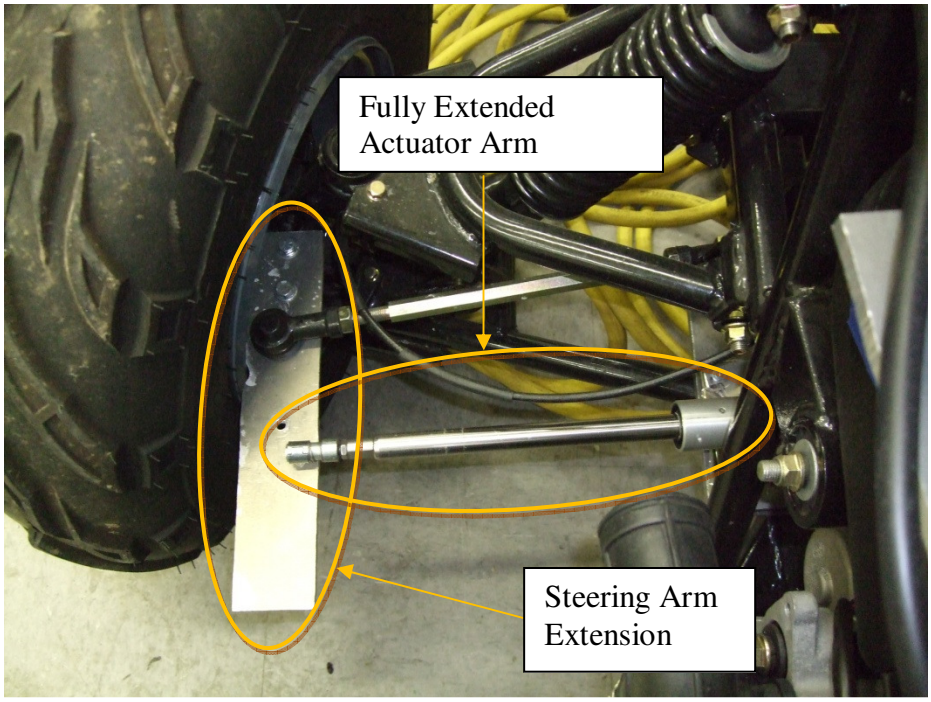

Figure 2.4: Steering linear actuator mounted on ATV frame.

This design does have its drawbacks, mostly relating to its interaction with the vehicle suspension. The movement of the suspension changes the distance from the

wheel to the central frame member of the ATV where the linear actuator is attached, changing the relationship between the actuator and the steering angle. In practice, this interaction between the steering angle and the suspension deflection makes controlling the ATV more difficult on rough terrain. This interaction can introduce high stresses into the system. In fact, the stud in the ball joint linkage at the end of the linear actuator broke after the ATV drove off of a curb. Fortunately, this vulnerability was easily mitigated afterwards by avoiding sharp elevation changes.

Overall, the steering system functioned well. Except for the aforementioned failure, the mounting system was compliant enough to avoid damage to the steering system due to rough terrain. The linear actuator proved to be powerful enough to steer the ATV over the entire range of motion in less than 3 seconds on any type of terrain.

2.1.2 Braking System

The ATV has two separate braking systems for the front and rear wheels. The front wheels have hand operated drum brakes. The rear wheels have a single hydraulic disc brake operated by a foot pedal. Due to the low ATV speeds expected during experimentation and for the sake of greater simplicity only the rear brake needed to be remotely controllable.

The braking is controlled with a linear actuator acting on the brake pedal. The linear actuator selected was a '4" Stroke 200 lbs Force Linear Actuator' sold by Firgelli Automations [10]. With a 12V supply, it has a no-load speed of about 0.75 cm/s with a maximum force output of 890 N. It only takes 360 N to fully compress the rear brake of the ATV, so this force output was more than sufficient. However, due to the slow speed of actuation, it takes the actuator at least two seconds to move the brake from fully released to fully engaged. Fortunately, since the ATV is intended to operate at low speeds in an open outdoor setting, quick braking is not necessary.

The linear actuator is attached to two mounting plates with factory-supplied brackets. The first mounting plate is attached to the top of the ATV frame just behind the gas tank. The plate is secured to the frame with U-bolts. The second mounting assembly consists of two plates that sandwich the factory installed brake pedal of the ATV.

Several bolts are positioned around the brake pedal in order to secure the plates to the pedal. The mounted linear actuator is shown in Figure 2.5.

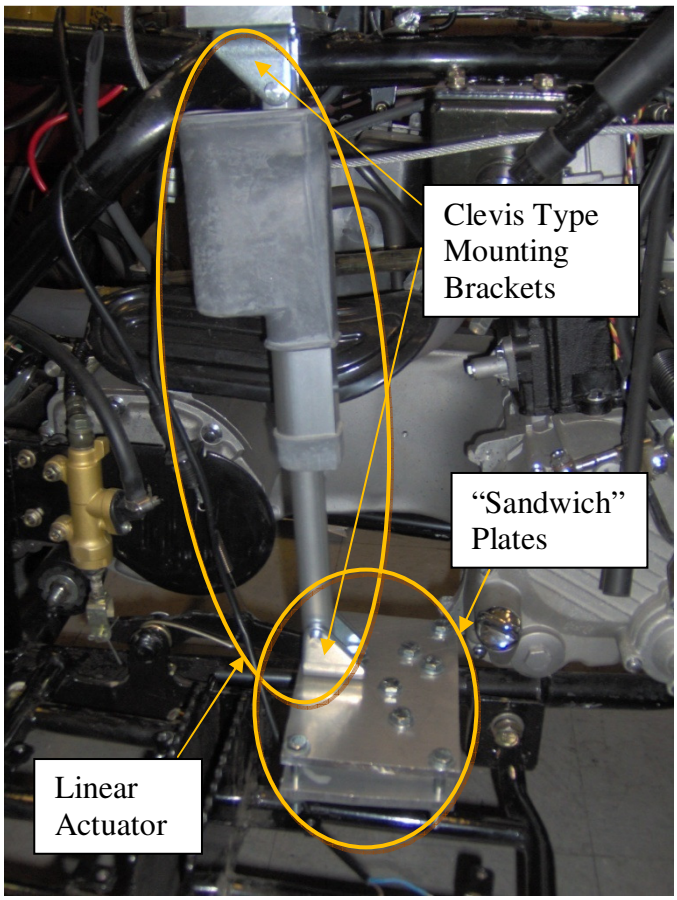

Figure 2.5: Mounted brake linear actuator.

The mounting components were placed in such a way that when the linear actuator is fully extended, the brake is very nearly fully compressed. Washers were added to the upper mounting bracket to fine tune the effective length of the actuator to allow the brake to compress fully. Because of this element of the design, there is no reason to have a lower limit switch associated with the linear. However, an upper limit switch is necessary to prevent the actuator from pulling the brake pedal past its fully released position and to reduce the amount of travel between the fully-open and fully-closed positions of the actuator. A normally open shoulder switch screwed onto an aluminum plate was installed on the foot well near the brake, as seen in Figure 2.6.

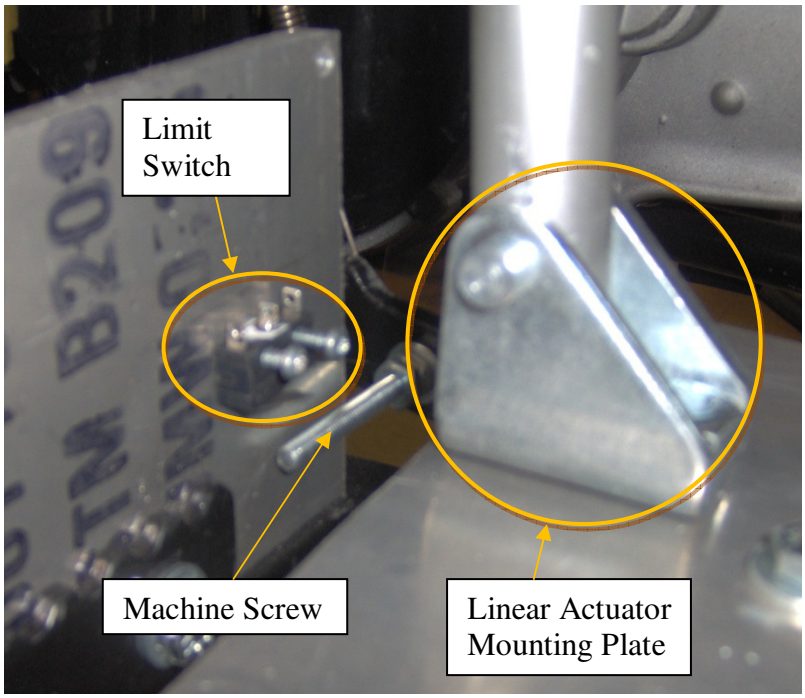

Figure 2.6: Brake actuator upper limit switch.

This aluminum plate is milled with vertical slots so that the position of the switch can be adjusted. A long machine screw attached to the brake pedal lever compresses the switch when the brake reaches its fully released position. This sends a signal to the braking actuator's motor controller to prevent the brake from moving further upward.

2.1.3 Throttle

The throttle of the ATV is controlled by turning the fuel valve on the carburetor. Normally the valve is pulled open by cable attached to a lever on the handlebars. The torque required to open this valve was measured over the entire range of operation of the valve. The maximum measured torque value was 0.6 N*m. In order to turn this valve, a servo was attached to the ATV underneath the fuel tank. The servo arm was attached to the fuel valve by a threaded rod with two clevis ends. This linkage is shown in Figure 2.7. The servo is a Hitec model HS-5995TG [11]. This servo is capable of producing a maximum of 2.35 N*m of torque when supplied with 6V.

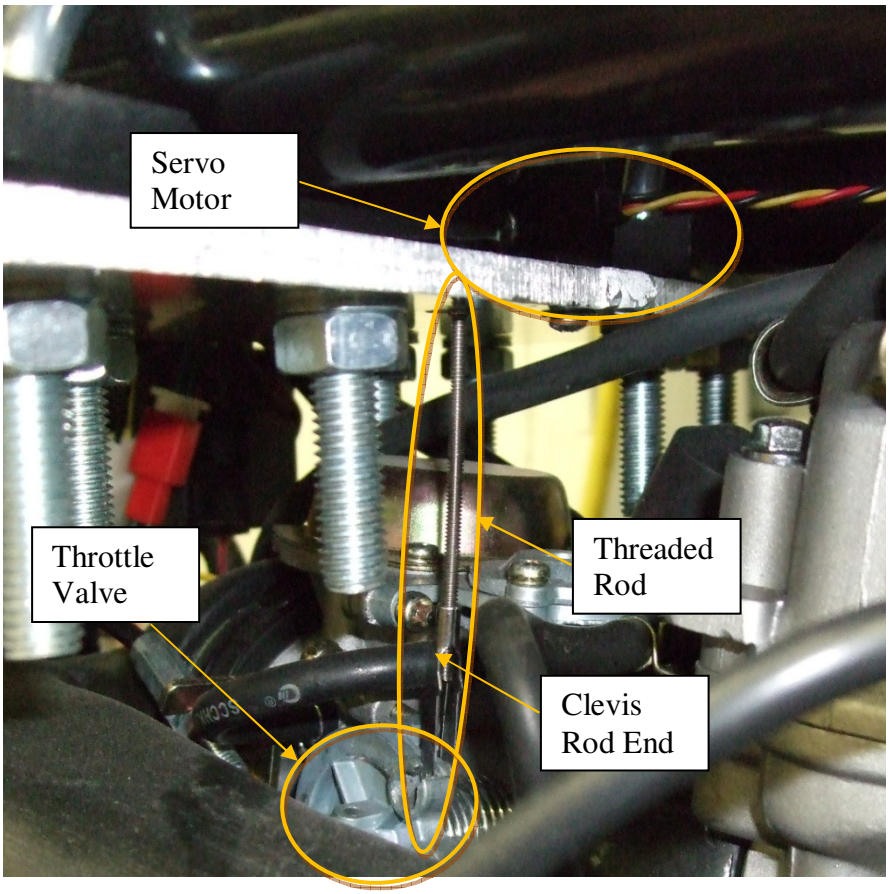

Figure 2.7: The throttle control linkage.

The linkage is assembled so that the threaded rod stays in a nearly vertical orientation. The length of the servo arm and the radius of the throttle valve are approximately the same. As a result, the motion of the throttle valve replicates the motion of the servo.

The servo is controlled directly by a square wave signal from a RC receiver, which is described in Section 2.2.1.

2.1.4 Remote Start

In order to facilitate easier experimentation in the field, a remote starter was added. Before modification, the ATV started by turning the key to the "ON" position,

engaging the rear brake, and pressing the start button. Under normal testing operation, the key is always left in the "ON" position and the rear brake can be remotely engaged. The starter button was simply replaced by a panel mounted switch that is located on the outside of the control box. A servo with a single arm attachment is mounted on the control box just above the start button so that the arm could contact the button. The servo is controlled and powered by the RC receiver, which is covered in Section 2.2.1.

2.2 Electrical Components

2.2.1 RC Transmitter and Receiver

Remote input to the system is provided by a remote control (RC) transmitter and receiver. The specific components used are a Hitec Optic 6 RC transmitter [12] and the Hitec Supreme 7-channel RC receiver [13]. The transmitter has a pair of two-axis joysticks along with and several buttons and switches. The receiver outputs a 0 - 3V square wave with a variable pulse width that depends on the RF (radio frequency) signal received from the transmitter. The transmitter can be programmed to adjust the upper and lower limits of the pulse width as well as the trim, or the offset of pulse width from the default setting.

2.2.2 Motor Controllers

Both linear actuators are controlled by Solutions Cubed Motion Mind 2 motor controllers [14]. This motor controller is capable of receiving multiple types of control input, including a square wave like the one produced by the RC receiver. The system is configured so that left-to-right movement of the transmitter's left stick steers the ATV to the left and right while up-and-down movement of the right stick engages and releases the brake.

The motor controller for the steering linear actuator operates in position-control mode with feedback from a linear potentiometer built-in to the linear actuator. The controller uses the RC input signal and the potentiometer feedback in a PID control

algorithm to control the linear actuator. The particular coefficients used with the algorithm were fine-tuned with repeated tests of the system.

The braking motor controller is also technically operated in position-control mode, but the system has been manipulated in such a way as to make it effectively a velocity-control mode. The position feedback channel on the controller receives a constant 2.5V input, which corresponds to a neutral position. Also, the integral, "I", and derivative, "D", coefficients for the PID algorithm are set to zero. When the control stick is in a neutral position, the linear actuator remains still, but when the control stick is moved backward or forward, the motor controller interprets the corresponding signal as a desired position. Depending on the displacement of the stick, the controller will supply a voltage to the actuator that either releases or engages the brake. In some cases, the braking linear actuator is controlled by the failsafe circuit, not the motor controller, and this is discussed in Section 2.2.3.

2.2.3 Failsafe System

The ATV is equipped with a failsafe system that is designed to keep the ATV from causing damage or injury should some aspect of the control system or wireless communication fail. If the failsafe does not receive a positive signal from a specific channel of the RC transmitter, it will cut off the engine, engage the brake and keep it engaged, and hold the steering in place. The channel that sends a signal to the failsafe is controlled by a switch on the transmitter. If this switch is flipped, the transmitter is turned off, or if the ATV goes out of the range of the transmitter, then the failsafe will engage after a delay of approximately 0.75 seconds. This delay is by design, in order to prevent momentary lapses in the signal or an interfering signal from engaging the failsafe. The circuit schematic is shown in Figure 2.8.

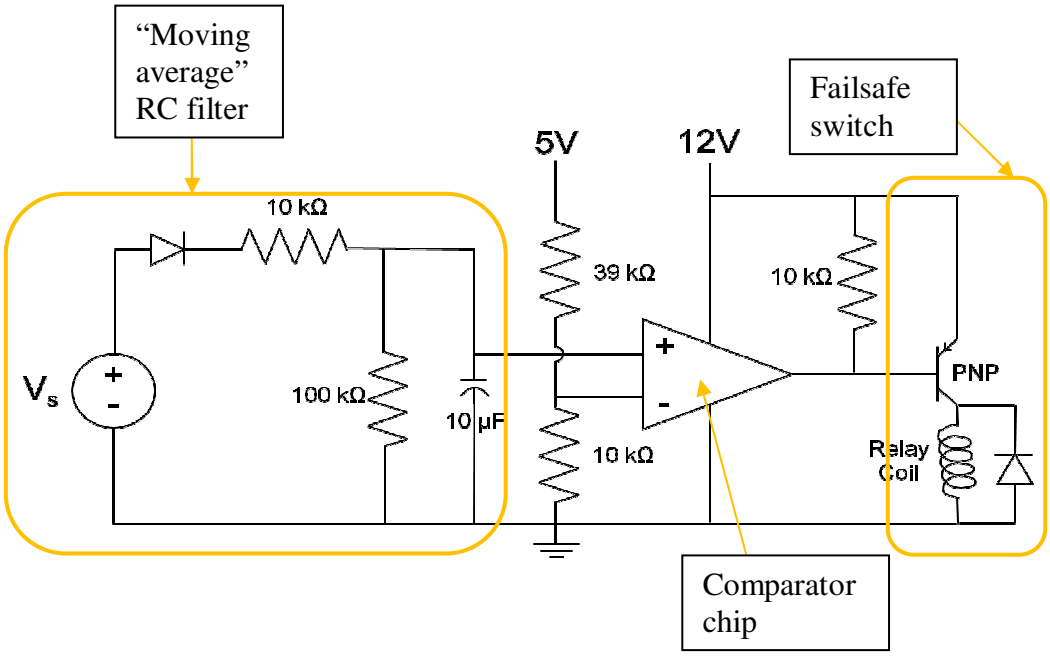

Figure 2.8: Signal-check circuit diagram.

The left side of the circuit effectively acts as a low-pass filter, providing a moving average of the square wave input by smoothing out the sharp changes in the signal. The circuit accomplishes this by employing two separate resistor-capacitor circuits at different times, depending on the state of the input signal. When the square wave input is at 3V (the "on" state), the 10 kΩ resistor and the capacitor form an RC circuit. In this case, the 100 kΩ is largely irrelevant, since it is in parallel with the capacitor. When the square wave input is at 0V (the "off" state), the 100 kΩ resistor and the capacitor form a different RC circuit as the 10 kΩ resistor is cut off by the diode. The output of this circuit is the voltage across the capacitor,

$$v_c(t) = V_i e^{-t/RC} \tag{2.1}$$

where V_i is the initial voltage, R is the resistance term and C is the capacitance term [15]. The RC term is commonly known as the "time constant" of the equation and it dictates

the decay rate of the capacitor voltage. Generally, a simple resistor-capacitor circuit reaches steady state after five time constants. The time constants of the "on" and "off" states of this particular circuit are 0.1 s and 1.0 s, respectively. Given that the pulse width and period of the signal are orders of magnitude less than the time constants, the sharp changes of the square-wave input signal are largely filtered out and the result is a moving average.

This moving average is compared to a DC reference signal. The level of the moving average depends on whether the transmitter switch is turned on or off. When the transmitter switch is turned on, the signal has an approximate pulse width of 2 ms. When the switch is turned off, the signal has a pulse width of 1 ms. The signal has an overall period of approximately 20 ms with a range of 0 to 3V, as discussed in Section 2.2.1. Testing showed that with the switch turned off, the resistor-capacitor component has a steady-state value of 0.80V ± 0.5V. With the switch turned on, it has a steady-state value of 1.25V ± 0.5V.

The comparator chip receives two inputs and varies its output depending on which input is higher. For this circuit, the second input is a 1 V reference signal, which is about halfway between the two steady-state values of the resistor-capacitor circuit. The output of this filter goes into a comparator chip. A comparator chip varies its output, either floating or pulling it to ground depending on which of two input signals is greater. Figure 2.9 shows a simulation of the signal check system being turned on, then the transmitter switch being turned off a few seconds later.

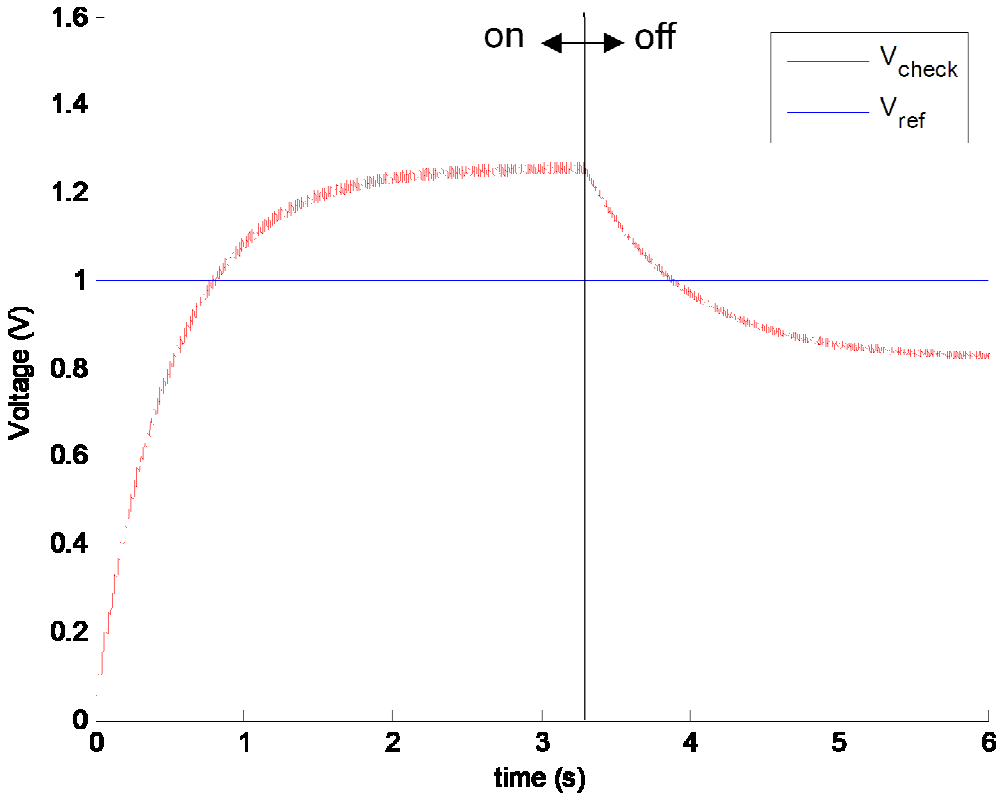

Figure 2.9: Simulation of signal-check circuit operation.

The graph shows the approximate initialization time of the circuit (the first second of operation), as well as the failsafe response time (after the on-off dividing line). The graph also shows that the adjusted signal has a steady-state amplitude of about 0.05V. This is due to the rapid switching of the square wave circuit, which the filter cannot completely remove. While no experimental data was recorded on the operation of the failsafe circuit, the simulation provides a fairly accurate estimate of these response times.

After the voltage across the capacitor and the reference voltage are compared, the output of the comparator chip is pulled up to 12V with a 47kΩ resistor. When the input from the RC receiver is higher than the reference input, the output of the comparator chip floats and is pulled to 12V. When the RC input is lower than the reference input, the output is pulled to ground by the chip. This output then feeds into the base junction of a PNP transistor. The circuit is designed for the transistor to operate in the "active region", where the transistor provides linear amplification of the input to the base junction [15].

This circuit only needs the transistor because the comparator chip alone cannot provide enough current to switch the relay.

Although the schematic only shows one relay, the transistor actually switches four relays: one for the ATV engine, one for the brake, one for the steering motor controller and one for an indicator LED. When the transistor receives 0V from the comparator chip, the relays revert to their normally closed (NC) state. When the relays enter this state, the voltage supply to the ATV engine becomes grounded and the engine cannot run or start. Also, the brake linear actuator connects directly to a 12V battery, causing the brake to close fully. Further, the "brake" input to the steering motor control is grounded, which prevents the steering linear actuator from moving. Finally, the failsafe indicator LED is turned off. When the transistor is receiving 12V from the comparator chip, the relays are activated and the normally closed terminals disconnect while the normally open (NO) terminals connect. In this state, the normal voltage supply to the ATV engine is restored, the brake and steering actuators are free to be manually controlled, and the indicator LED for the failsafe is turned on.

Because of the ability of the failsafe to stop the engine, it is useful as more than just a safety feature. Some of the tests involve moving the ATV then stopping the engine to record data. When combined with a remote start mechanism, the user gains the ability to remotely start and stop the ATV's engine.

2.2.4 Signal Buffers

In order to protect the integrity of the signals going from the RC transmitter to the two motor controllers, the signals were sent through a pair of cascaded buffer-amplifiers. Before the buffers were installed, the actuators often behaved erratically and suffered from unpredictable outbursts of jittering. The instruction manual for the Motion Mind controllers indicated that if the system experienced this behavior and the peak-to-peak amplitude of the square wave input signal was less than 5V, then adding buffers could alleviate the problem. The brake and steering signals coming from the RC receiver have amplitudes of approximately peak-to-peak 3V. Since the buffers used, Texas Instruments

hex buffers, cannot amplify the signals from 3V to 5V, a pair of buffers are cascaded for each channel. The first set of the buffers bring the signals to 4V peak-to-peak amplitude while the next set amplifies to the full 5V peak-to-peak amplitude recommended by the motor controller documentation [14]. Figure 2.10 shows the circuit diagram for the signal buffers.

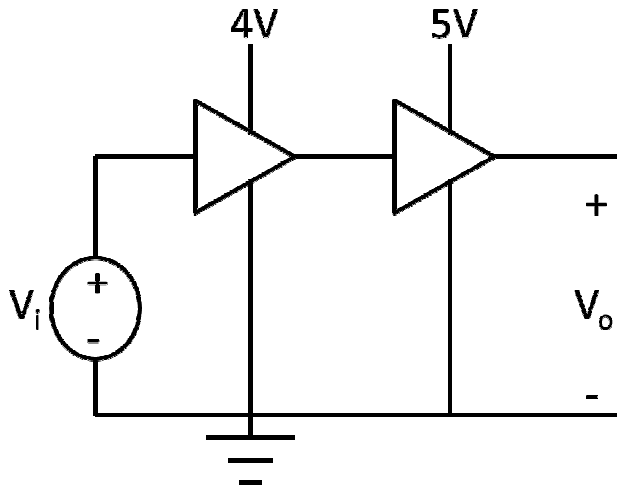

Figure 2.10: Circuit diagram of cascaded signal buffers.

Overall, the addition of the signal buffers had a positive effect on system performance. However, it appears that some of the problems experienced by the system come from cross-channel signal interference. It is uncertain how much of the interference was between the receiver channels and how much was from an exterior source.

2.2.5 Control Packaging

Most of the control hardware for the remote control is packaged inside an ABS plastic box mounted just behind the fuel tank of the ATV. Inside this box are the motor controllers for both the steering linear actuator and the brake linear actuator, the failsafe circuitry, fuses, and signal buffers. On the outside of the box are located several

switches, a signal indicator light, an engine starter button and a servo to press the engine starter button. A view of this packaging can be seen in Figure 2.11.

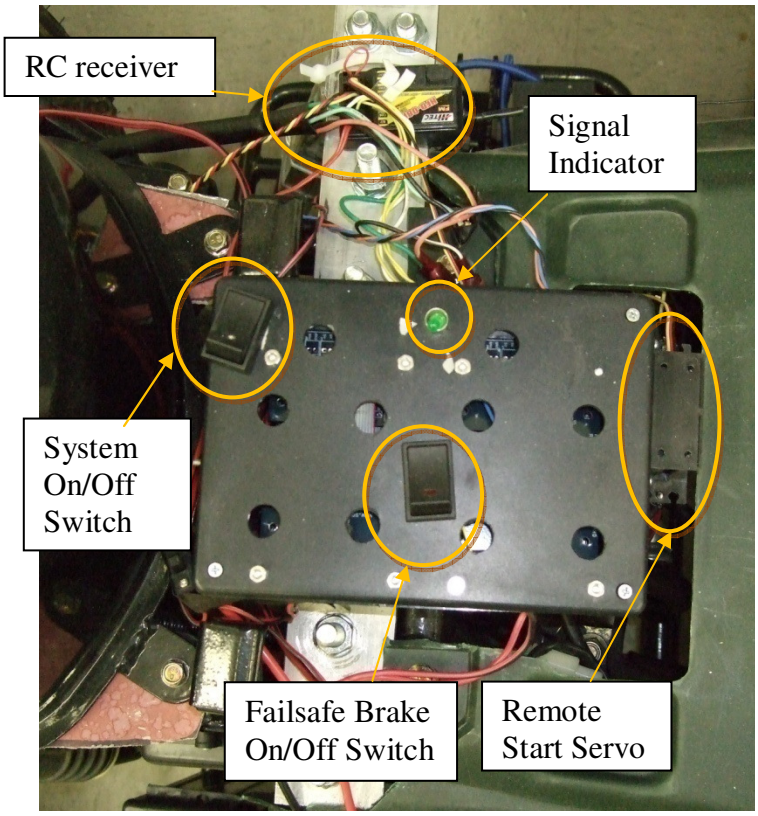

Figure 2.11: ATV Control Package.

The RC receiver is placed outside of the control box to minimize interference between the receiver and the motor control boards.

Chapter 3: ATV Instrumentation

The primary function of the ATV is to function as a mobile sensor platform. While many more sensors and instrumentation can be added to the platform, this section will detail the sensor hardware that has already been installed on the ATV. The added instrumentation includes a compass, a GPS receiver, microphones, accelerometers, analog filters and embedded computers. A fully outfitted vehicle can be seen in Figure 3.1. Figure 3.2 shows a schematic of the instrumentation system.

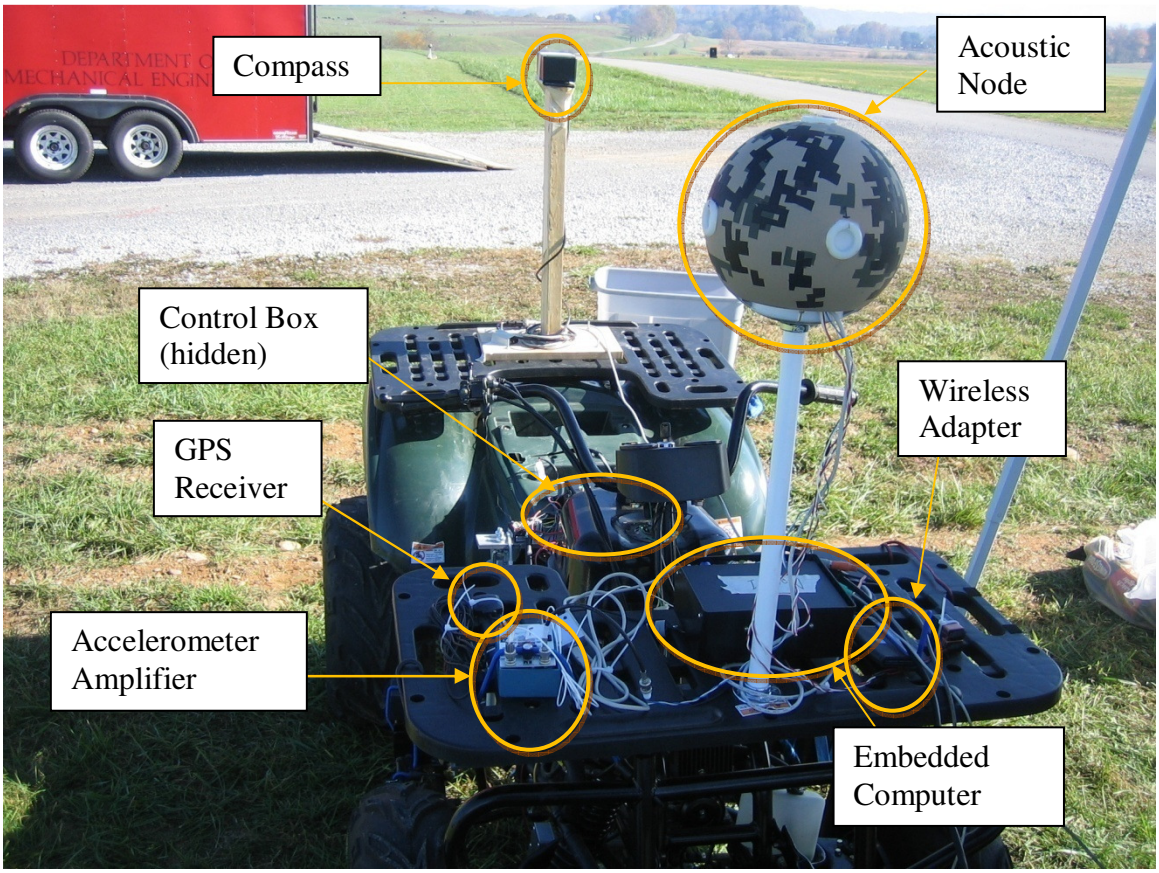

Figure 3.1: ATV Instrumentation (camera and servo controller not shown).

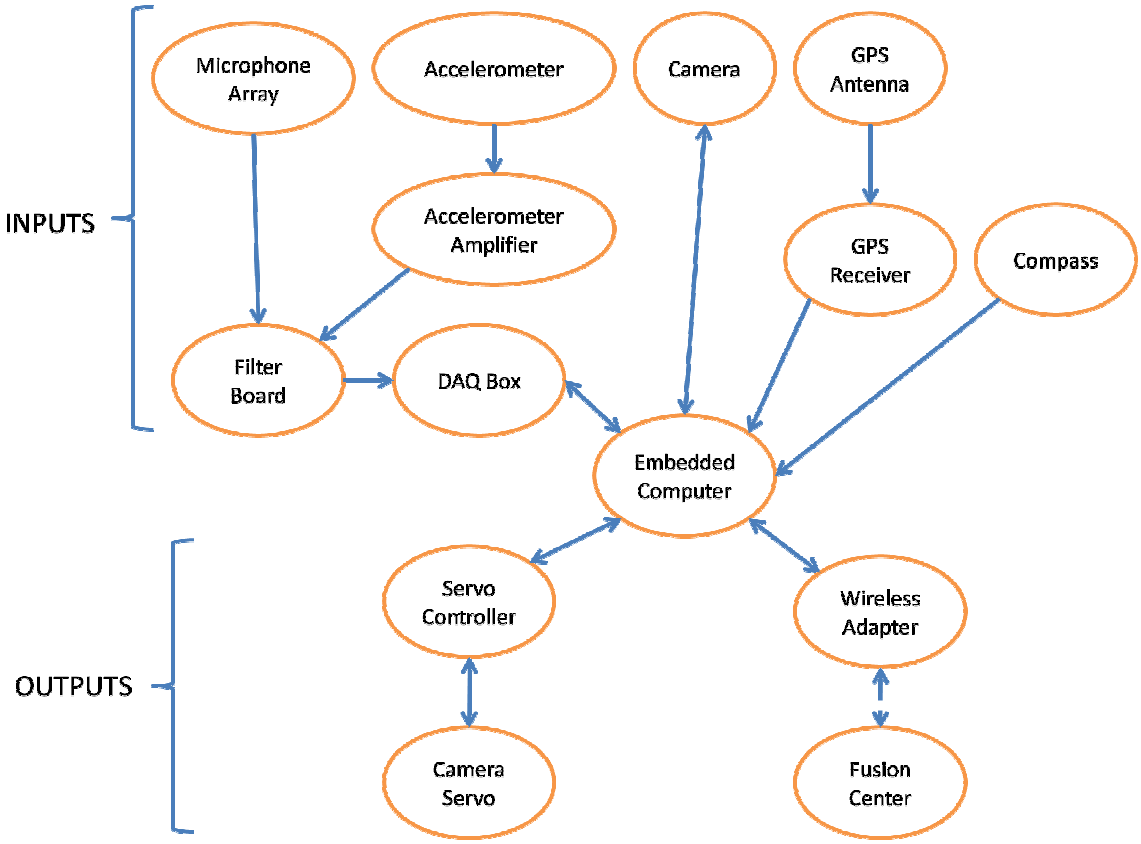

Figure 3.2: Instrumentation schematic.

3.1 Embedded Computer

The computer used for data processing and network communication is a Sealevel Relio R1220 Industrial Computer [16]. This computer contains a 1.0 GHz Intel Processor with 512 MB of RAM and a 30 GB extended temperature hard drive. The unit measures 7.5" x 5.1" x 1.8" and weighs approximately 1.0 kg. This computer was selected due to its durability and small size and very low power consumption.

During initial testing, the computer would frequently crash while the engine was running. A vibration isolation mount for the computer was then designed and installed. Designing the vibration isolation system required some knowledge of the actual vibration experienced by the embedded computer. An accelerometer placed on the front equipment rack of the ATV served to estimate vibration experienced by the embedded computer. The lowest frequency of engine vibration seen by the accelerometer was

approximately 13 Hz when idling. However, most problems in the field occurred when the engine was running at half-throttle or greater, so multiple engine speeds were tested. Figure 3.3 shows several frequency domain plots of the engine vibration at different engine speeds.

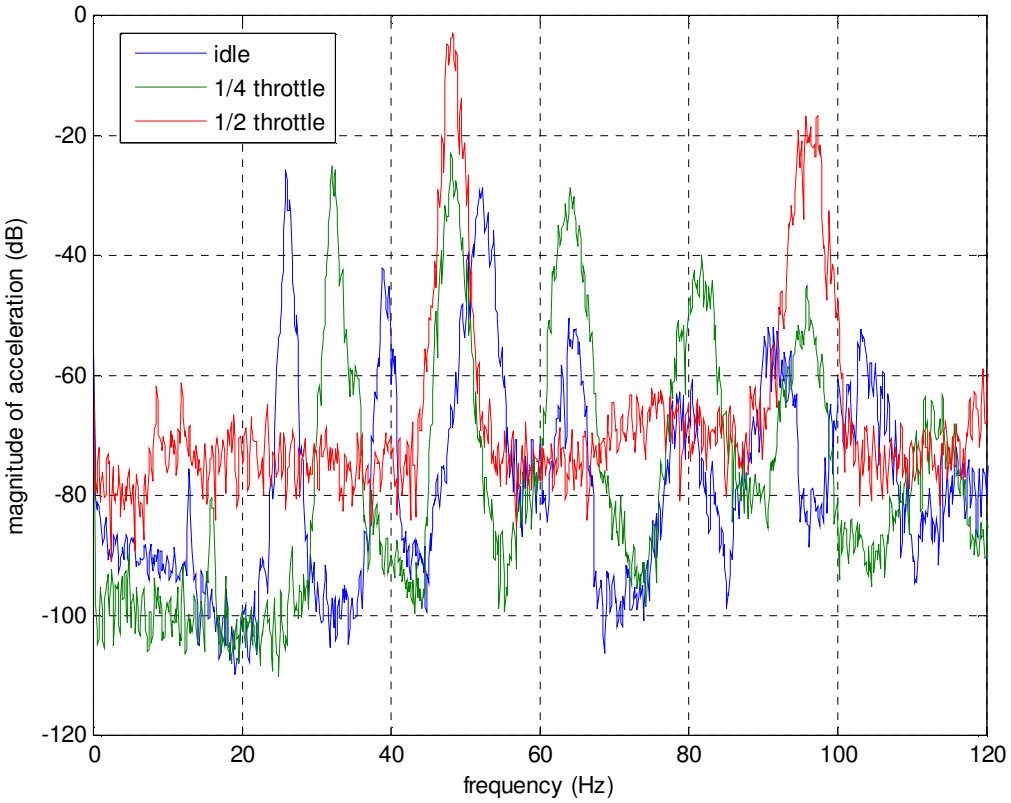

Figure 3.3: A comparison of the frequency content of the vibration seen by the embedded computer at engine idle and ¼ and ½-throttle.

The frequency plot indicates that the primary frequencies of the transmitted engine vibration are approximately 13 Hz, 16 Hz and 48 Hz, for idling, quarter-throttle and half-throttle, respectively. Subsequent peaks on the graph indicate the harmonics of each primary frequency. The frequency responses lack sharp, well-defined maxima because the frequency of engine tends to oscillate over time. This behavior is most noticeable in harmonic frequencies visible in the graph range.

The goal of the vibration isolation mount is to mitigate the effects of engine vibration at higher engine speeds while not exacerbating them at lower engine speeds. For the purposes of this design, higher engine speeds were considered to be half-throttle and above, where most of the computer problems were experienced.

For this vibration isolation mount, the computer was mounted into a Radio Shack plastic project box measuring approximately 8" x 6" x 4". This enclosure was attached to the front ATV equipment rack by three bubble isolation mounts. The computer is shown mounted in Figure 3.4.

Figure 3.4: Embedded computer shown mounted on ATV front rack.

The isolation mounts have a quoted deflection of 0.12 inches with a load of 18 pounds. Assuming a linear stiffness, this is equivalent to 54.2 pounds/inch or 9.47 kN/m. The three mounts together had an effective stiffness of 28.4 kN/m and are considered the only non-rigid members of the system. The computer is installed in the top of the box and 12 brass weights weighing a total of 2.5 kg are placed in the bottom of the enclosure. Modeling clay weighing approximately 1.0 kg occupies the vacant space at the bottom of the enclosure to secure the brass weights and add more weight. The plastic enclosure and the screws used to secure the computer in the enclosure contribute a negligible amount of weight. Together, all of the components inside the plastic enclosure weigh approximately

4.50 kg. In considering the dynamics of this system, all potential vibration modes other the first mode (simple up-and-down motion) are ignored. The natural frequency of an undamped single-degree-of-freedom oscillator

$$\omega_n = \sqrt{\frac{k}{m}} \tag{3.1}$$

where k is the effective stiffness of the spring members and m is the mass of the oscillating body. This gives us a natural frequency of 79.4 radians per second or 12.6 Hz.

In order to confirm the vibration isolation of the system, the transmissibility equation can be used. The ratio of input force to output force in a vibration isolation system, also known as the transmissibility ratio

$$TR = \frac{\sqrt{1+(2\zeta\omega/\omega_n)^2}}{\sqrt{[1-(\omega/\omega_n)^2]^2+[2\zeta\omega/\omega_n]^2}} \tag{3.2}$$

where ζ is the damping ratio, ω is the forcing frequency of the vibration source, and ω_n is the undamped natural frequency of the system [17]. The forcing frequencies of the engine and the natural frequency of the system are known, but the damping ratio is unknown. Regardless of the damping ratio, the system can be considered to be isolated when $\omega/\omega_n > \sqrt{2}$. The ratios of forcing frequency to undamped natural frequency at idle, quarter-throttle and half-throttle are 1.03, 1.27 and 3.81, respectively. If the system was undamped or very lightly damped, significant amplification would be expected at idle speed and moderate amplification would be expected at quarter-throttle. However, the damping in the system would somewhat mitigate the amplification seen at low engine speeds. Fortunately, no problems with the computer operation were seen at low speeds, with or without the vibration isolation system.

To validate the effect of the vibration isolation system, the measured attenuation of the system can be compared to the transmissibility ratio described in Equation 3.2. The maximum theoretical attenuation for a given frequency ratio can be found by assuming the damping ratio in Equation 3.2 to be zero. This reduces the transmissibility ratio to

$$TR = \left|\frac{1}{1-(\omega/\omega_n)^2}\right| \tag{3.3}$$

For the frequency ratio at half-throttle, 3.81, the transmissibility ratio is 0.074. This is equivalent to an attenuation of 22.6 dB. The actual attenuation gathered from experimental data is demonstrated in Figure 3.5.

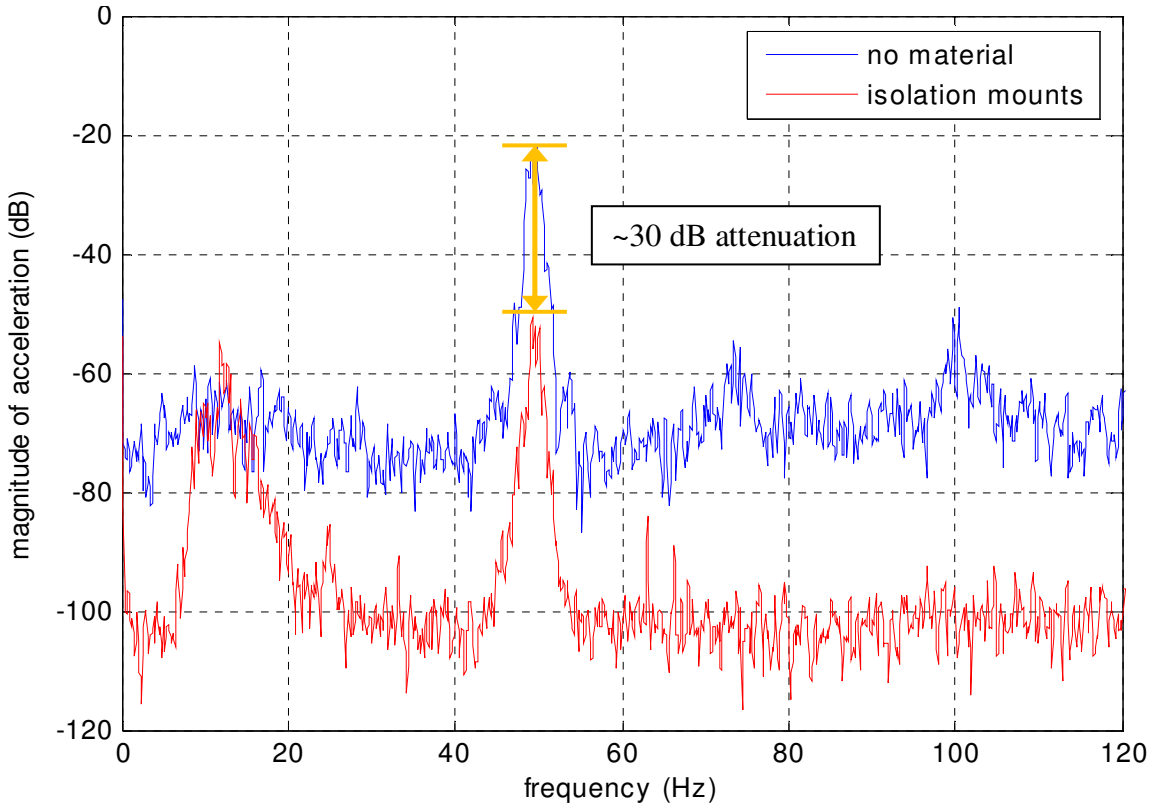

Figure 3.5: Comparison of engine vibration at half-throttle between a rigidly mounted computer and the vibration isolated computer.

At half-throttle, the transmitted engine vibration appears to be reduced by as much as 30 dB, more than the theoretical maximum. At higher speeds, even more attenuation should be seen. This isolation was significant enough in practice to effectively eliminate interruption of the computer due to vibration.

3.2 Acoustic Node

The acoustic node is the most important sensor in the system and the inspiration for creating a mobile sensor platform. It consists of a five-channel microphone array, a pre-amplifier/filter circuit board and a data acquisition box all contained within a hollow plastic sphere. Put together, these components transmit five acoustic signals to a matlab-based interface called "Node Processor". Both the Matlab code and the acoustic node system were designed by Philip Gillett and are described in greater detail in his doctoral thesis [1]. This section will briefly describe the components in this system. This node is attached to the front equipment rack of the ATV with an approximately 30 in. long pole, as shown in Figure 3.6.

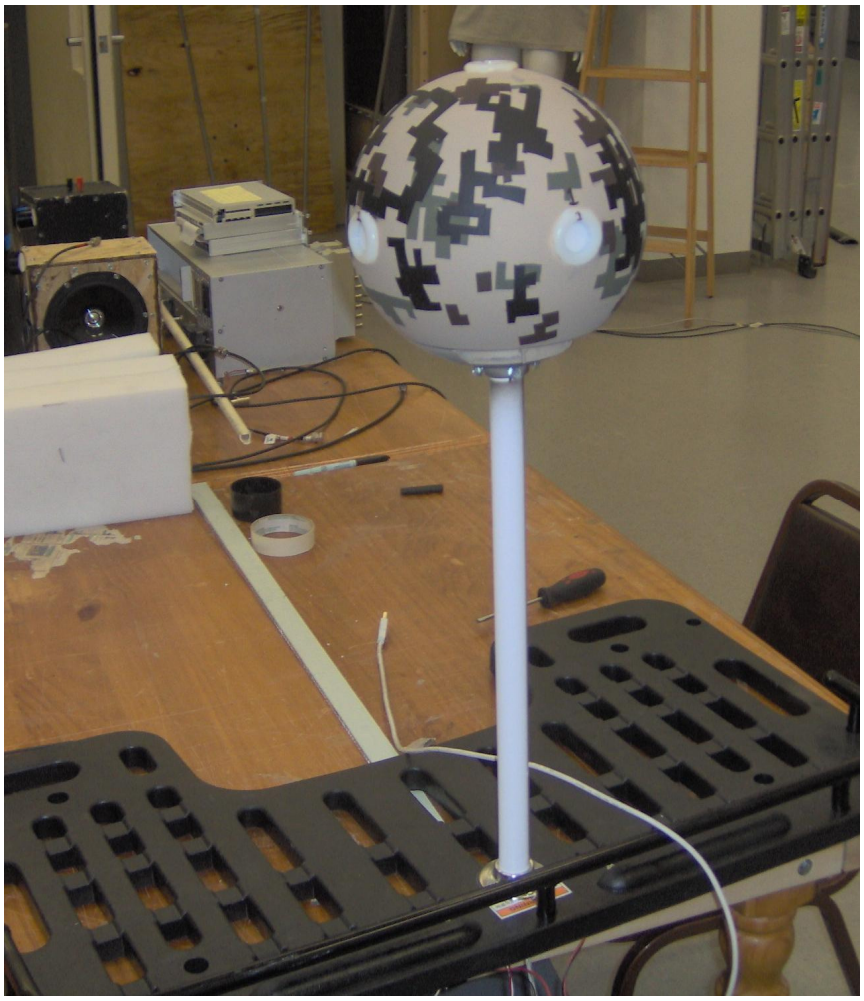

Figure 3.6: 5-microphone array shown mounted to front equipment rack.

3.2.1 Microphone Array

The microphone array consists of five condenser microphones covered with foam and placed in custom manufactured mounts designed by Dan Mennitt. The foam serves to lessen the effect of wind on the microphones. The microphone mounts are evenly spaced on the plastic sphere with one on top and four around the equator of the sphere. The sphere is lined with foam to dampen any potential resonance. Figure 3.7 shows the location of the microphones on the sphere.

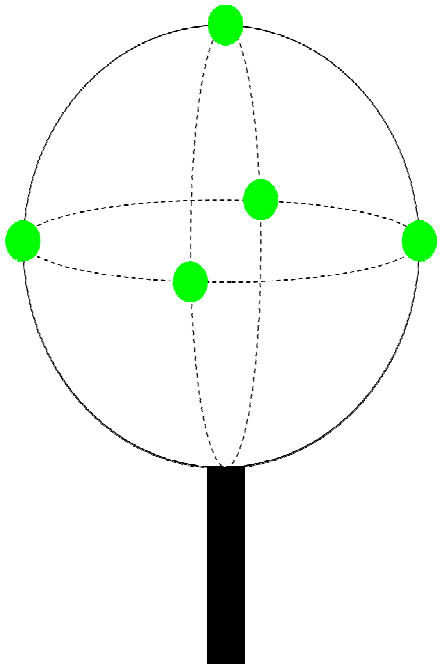

Figure 3.7: Location of microphones on hollow plastic sphere.

3.2.2 Filter Board

The pre-amp/filter board powers the microphones and filters their signals. The bandpass filter consists of a highpass RC filter with a cutoff frequency of approximately 100 Hz and a 4-pole Chebyshev low-pass anti-aliasing filter set at approximately 3000 Hz. The array is designed to sample at 8192 Hz. The board also contains potentiometers to adjust the gain of each microphone.

3.2.3 Data Acquisition Module

The data acquisition module (DAQ box) is a Data Translation Econ Series DT-9816 [18]. It has six simultaneously sampled analog-to-digital convertors as input. The unit has a software adjustable sample rate up to 50 kHz. Throughout testing, the sample rate was set to 8192 Hz. Five of the channels are devoted to the microphone array while one is used for the reference accelerometer which is discussed in section 3.3. The DAQ box connects to the embedded computer with a USB interface.

3.2.4 System Characterization

The node is used along with minimum variance distortionless response (MVDR) beamforming to estimate the direction of an acoustic source. In order to implement this approach, the system must first be characterized in an anechoic chamber. For this process, the microphone array and filter board were placed on a stand that allowed the array to rotate freely. The Data Translation DAQ box was replaced with a National Instruments data acquisition system to sample the acoustic signals. A speaker directed at the array produced with noise for approximately 30 seconds. After each test, the array was rotated in 15 degree increments, for a total of 18 different azimuth angles. After a set of azimuth angles was completed, the elevation angle of the noise source increased by 20 degrees, from 0 to +80 degrees, for a total of five elevation angles. These tests create a series of transfer functions that are later used to determine the angle and frequency composition of a noise source in the field.

3.3 Reference Accelerometer

The obvious difficulty of trying to perform acoustic localization on an ATV is the presence of loud engine noise which will dominate any other noise received by the microphones in the acoustic node. One way to eliminate a known source of interference

such as an engine is to use least mean square (LMS) filtering. The LMS filtering process uses a measurement of the known interfering source and filters it from a mixed signal leaving everything but the interference [19]. This should allow for the acoustic node to effectively ignore the engine noise when listening for acoustic sources. The LMS filtering algorithm is discussed in detail in Section 4.3.

In order to get a measurement of the engine noise, an accelerometer was attached to the transmission case of the ATV. The mounting location is highlighted in Figure 3.8.

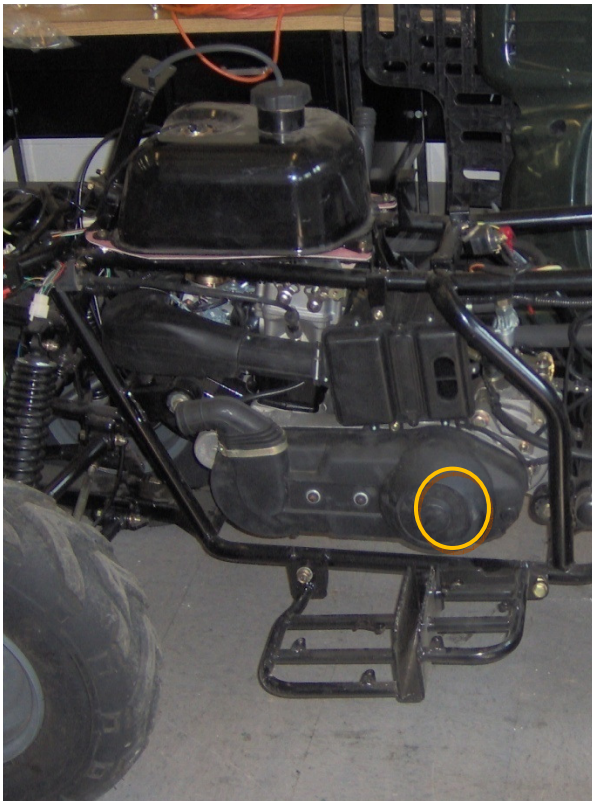

Figure 3.8: Mounting location of accelerometer.

The transmission case is rigidly attached to the engine and so the accelerometer placed on it will approximate the acoustic noise produced by the engine.

3.4 GPS

A number of different GPS units were evaluated and tested for use including the Garmin 18USB GPS Receiver and the Wintec WBT 201 GPS Recevier/Data Logger. Both of these units performed adequately in testing, but ultimately an AuSIM GPS2 receiver was installed with a Trimble miniature 5V GPS antenna.

The AuSim GPS receiver interfaced with the embedded computer through included software. This software emulated a serial port which was scanned periodically by the Matlab node processor program for location information. The receiver reported position in latitude, longitude, and altitude, as well as the geometric dilutions of precision (DOP) of each dimension.

3.5 Compass

An electronic compass is used to determine the orientation of the ATV. A PNI TCM 2.6 module was used for this purpose [20]. The TCM 2.6 is a 3-axis tilt compensated compass, meaning that it has three orthogonal magnetometers and two orthogonal accelerometers to measure the nearby magnetic field in 3 dimensions and measure the orientation of the compass with respect to the ground. This enables the module to get an accurate bearing when it is not level. This particular model can be tilted up to 50° from horizontal. This module samples at a rate of 8 Hz and when properly calibrated has an accuracy of 0.8° RMS over its entire tilt range. The TCM 2.6 communicates through a serial connection. The node processor program scans this port in the same manner as the GPS unit to extract heading information.

The calibration process will remove the effect of permanent magnets, or “hard iron effects” which have a constant magnetic field. However, the calibration process can not compensate for the presence of ferrous metals, or “soft iron effects”, which can alter magnetic fields that pass through them. Therefore, the compass is mounted on top of a wooden beam far away from the ATV’s steel frame or any other ferrous metal. This arrangement can be seen in Figure 3.9.

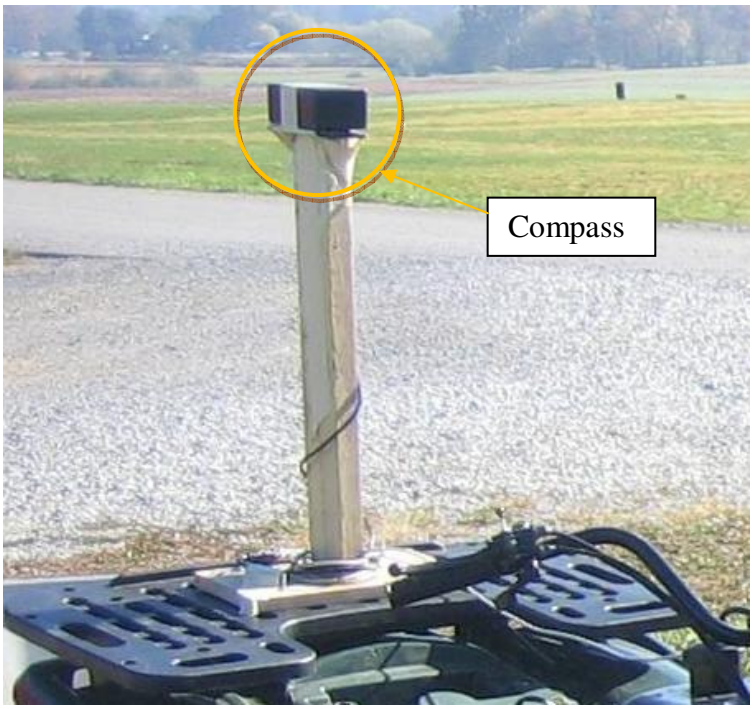

Figure 3.9: Compass mounted on rear equipment rack of ATV.

The calibration process calls for the module to be firmly mounted, then be rotated twice while being tilted at different orientations. Since rotating and tilting the entire ATV is very impractical, the rear equipment rack of the ATV is detached and, along with the wood beam and compass, rotated and tilted while the calibration feature of the compass software is running.

3.6 Camera

A camera is attached to the front of the front equipment rack in order to record visual data of events triggered by acoustic detection. The camera is a generic clip-on webcam measuring approximately 2.5 cm x 4 cm x 4 cm. The camera is capable of up to 800 x 600 pixel resolution and up to 24-bit color resolution. It is equipped with a manual focus.

The camera mounts on a servo arm so that it can pan left and right to capture images over a large field of view. The servo is a Hitec HS-311 which has an

approximately 180° range of motion. The servo is powered and controlled by a Lynx Motion SSC-32 Servo Controller. The controller processes commands from the onboard computer via a serial interface. When the camera is mounted on the servo, it can travel 180 degrees in approximately one second. The camera and servo are shown mounted in Figure 3.10.

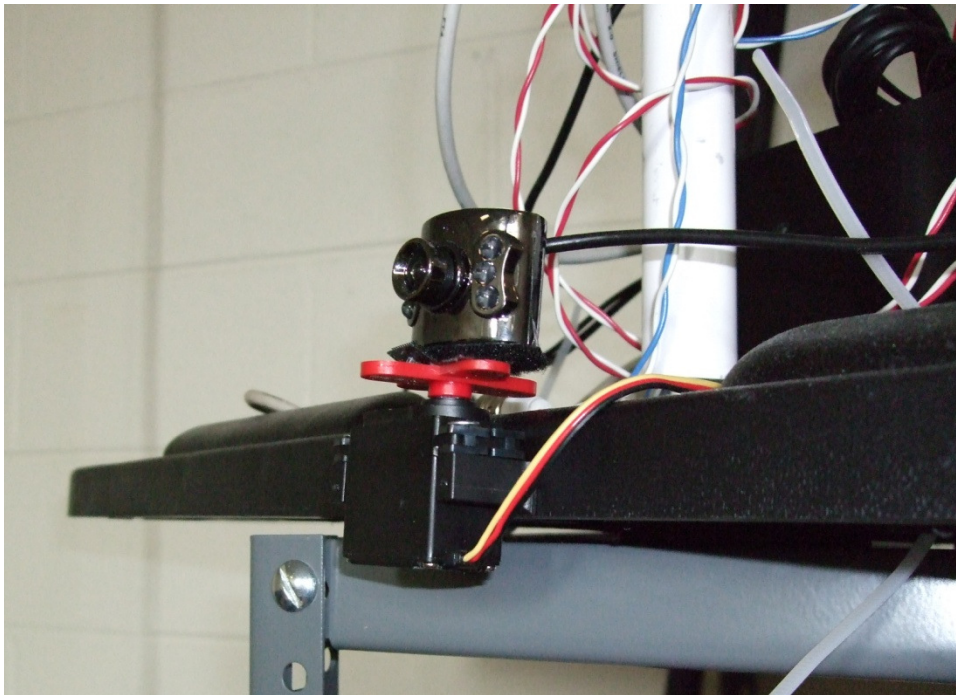

Figure 3.10: Camera mounted to servo.

The computer receives images from the camera through AbelCam webcam server software. This allows the camera to be running continuously while the computer saves or processes images only whenever requested.

3.7 Wireless Adapter

A Linksys USB Wireless Network Adapter WUSB54G provides wireless communication. It uses the 802.11g wireless protocol, communicates with the computer using a USB connection, and is equipped with a small adjustable antenna. During

experimentation, it had a range of at least 50 m when used in conjunction with a Linksys Wireless-G Broadband Router with high gain antenna.

3.8 Node Processor

The embedded computer uses a Matlab-coded interface named "Node Processor". This program was coded by Dan Mennitt and Philip Gillett. This program has the capability to gather acoustic data in pseudo-real-time and determine the incidence of tonal and impulsive acoustic events. The program will then condense this data into packets called "feature vectors" and transmit them to a central computer ("fusion center") running the Matlab-based "Fusion Center" code written by Dan Mennitt. Each Feature Vector contains the direction of the source, as well as the frequency of the source for tonal sources, and the exact time of detection for impulsive sources.

The Node Processor code can also interface with the GPS and compass units described in Sections 3.4 and 3.5. If these units are implemented for a particular node, stationary or mobile, Node Processor will continuously sample them and include location and orientation data with each feature vector. If these units are not implemented, Node Processor will transmit a set position and orientation with each feature vector.

Chapter 4: Component Testing

Several tests in different environments were conducted to demonstrate the effectiveness of this mobile sensor platform. Each sensor component was tested separately to determine the effectiveness of its implementation. The tested components detailed in this section include the GPS receiver, the electronic compass and the engine accelerometer.

4.1 GPS

4.1.1 Stationary Testing

The effectiveness of the GPS unit was validated in several experiments. The GPS receiver was first tested for consistency over time. One problem with a GPS unit is signal drift. Due to atmospheric conditions and other sources of interference, the estimated position of the GPS unit can change over time even when it is stationary. Drift can be compensated for, but not without the addition of a costly inertial measurement unit (IMU). Therefore, it is necessary to be able to quantify the amount of signal drift. Other tests were conducted to test the accuracy of the recorded path of the GPS unit with respect to a fixed reference point.

In order to test the GPS unit's signal drift, the unit was attached to a computer and left to acquire position coordinates for approximately forty minutes. Figure 4.1 shows the values of the easting and northing coordinates over time. The origin of this graph is the initial GPS measurement. The estimated position of the unit varies by no more than two meters in any direction.

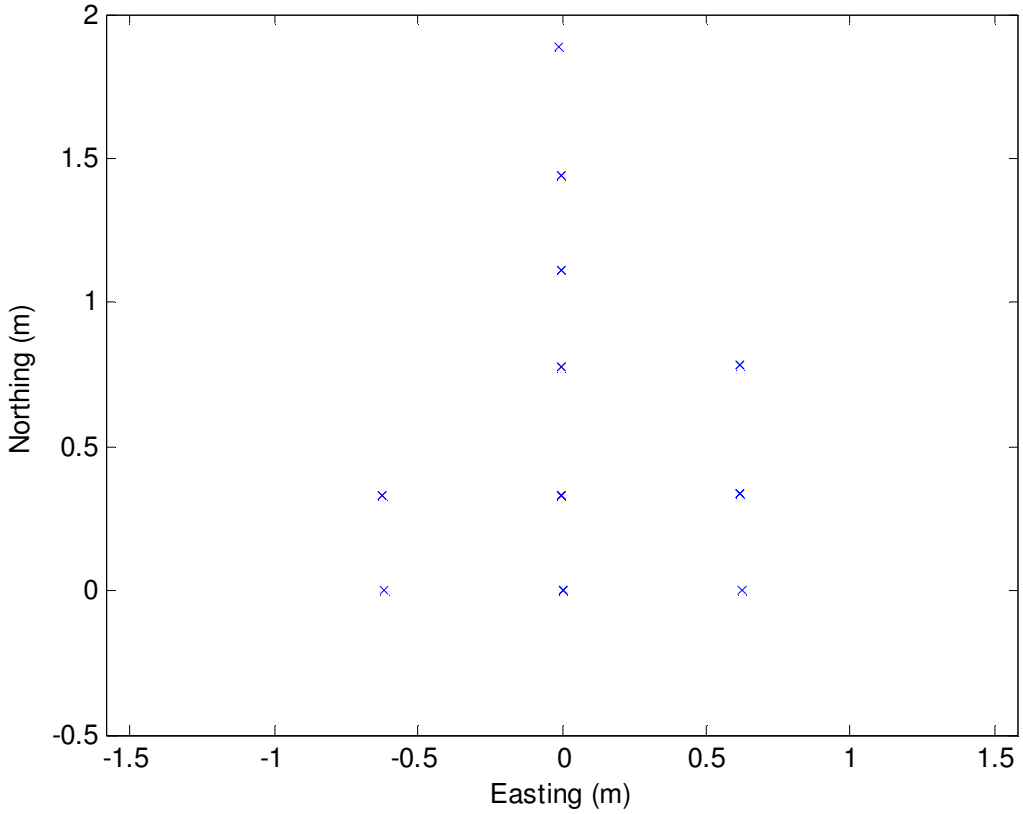

Figure 4.1: GPS measurements over 40 minutes showing signal drift.

Typical test runs for acoustic localization ranged from two to ten minutes. It is assumed that the signal drift during a typical test will be less than this amount. However, over a longer period of time, drift could become a more significant problem. In order to mitigate the effect of long-term drift, the positions of all nodes, mobile and stationary, were sampled during each test.

4.1.2 Mobile testing

Multiple tests of the GPS receiver were undertaken to ensure that the GPS unit functioned reliably. The intention of these tests was not to measure the accuracy of the GPS unit, but to test the ability of the AuSim software to record GPS data and to determine the quality of the GPS data.

In order to have a frame of reference, the tests were generally conducted on roads and paths with known GPS coordinates. One such test was conducted at the primary test site at Kentland Farms, land owned by the Virginia Tech College of Agriculture and Life Sciences and used primarily for agricultural research. While GPS-recording code ran on the embedded computer of the ATV, the ATV was driven down a gravel road running through the test area. The coordinates of the test area were interpolated from a large map of the area bounded by known GPS coordinates. Figure 4.2 shows the results of this test.

Figure 4.2: The track of the ATV during a test run as recorded with the GPS unit.

The GPS track of the ATV closely follows the path of the gravel road with little error and no noticeable outliers. The small error that exists is likely a result of the GPS receiver's limited precision. Similar tests conducted in Kentland Farms and other locations generated similar results. Given that the gravel path was between two and three meters wide, the GPS system could be counted on to provide the path of the ATV within a meter most of the time.

4.2 Compass

The measurement of the ATV's orientation with the electronic compass proved to be problematic. When the ATV's engine was running, the compass returned meaningless data that varied wildly even when the ATV was not moving. The most likely source of this behavior was the combination of the ATV's engine vibrations and the compass's tilt compensation feature. As previously mentioned in Section 3.5, the compass uses two accelerometers to allow for tilt compensation. These accelerometers are intended to measure the pitch and roll angles of the compass and allow it provide a reliable heading even when it is tilted at a large angle. When the ATV is running, the integrated accelerometers may pick up the engine vibrations. This results in the measured tilt of the compass unit varying greatly and being completely unreliable. Unfortunately, the compass interface did not allow for the tilt compensation feature to be disabled. The serial interface between the compass and the embedded computer does not allow direct measurement of the accelerometer signals, so the reference accelerometer (Section 3.3) was used to compare the engine vibration with the reported compass heading. Figure 4.3 shows this comparison.

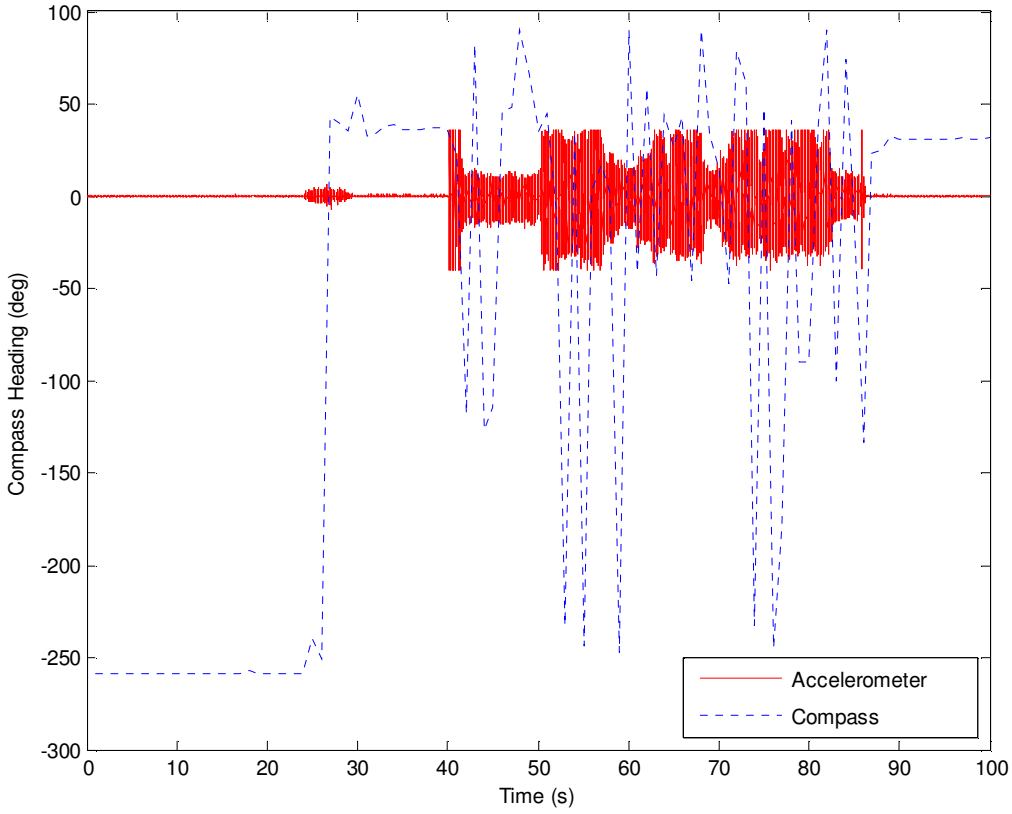

Figure 4.3: Time plot of compass bearing and engine acceleration.

The sections of the graph where the compass heading has large variations coincide with the time when the ATV's engine is running, which is indicated by a noticeable accelerometer signal. When the engine is turned off, the compass's orientation measurement is predictably stable.

4.3 LMS Filtering

The reference accelerometer, as explained in Section 3.3, is included in the ATV instrumentation package to allow for LMS filtering of the engine noise. The goal of the LMS filtering is to allow the node processor to localize acoustic sources while the ATV's engine is running. While tests of the algorithm looked promising, the algorithm was never successfully used with the node processor algorithm.

LMS filtering is an adaptive algorithm that attempts to remove interference from a signal by using a reference signal of the interference. The algorithm uses a finite impulse response (FIR) filter that is automatically adjusted depending on the reference signal and the output signal, also called the error signal [19]. In this application, the system experiencing the interference is the acoustic array, the interference is the noise from the engine, and the reference signal is gathered from the accelerometer.

Several trials were conducted to develop and test the LMS algorithm. During these trials, the acoustic node attempted to locate an acoustic source while the ATV's engine was running. Comparing the data from the accelerometer and the rear-facing microphone illustrates the potential effectiveness of the algorithm. Figure 4.4 shows some of the raw data collected from each source.

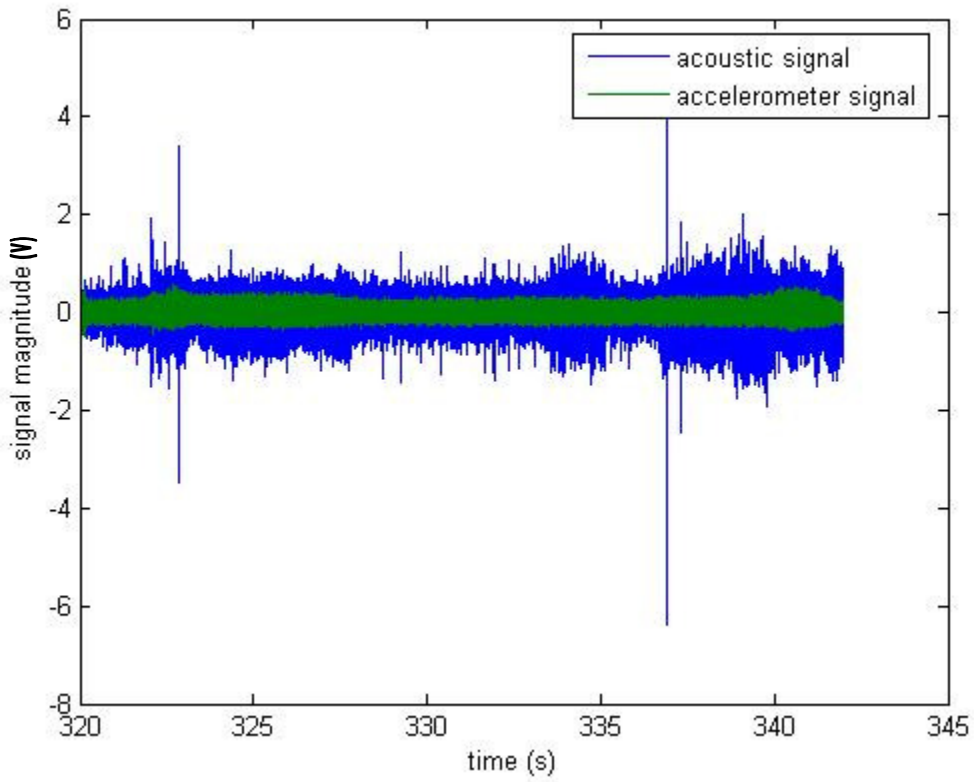

Figure 4.4: Accelerometer signal and microphone signal taken with running ATV engine.

While both signals show a persistent engine noise component, the acoustic signal has several spikes that exceed the base noise level. These spikes represent impulses

generated with a cap gun that the acoustic node is attempting to locate. To further compare the two signals, Figure 4.5 and Figure 4.6 show, respectively, power spectral density plots for both signals in the entire measured frequency range (0 to 4096 Hz) and a low frequency range (0 to 500 Hz).

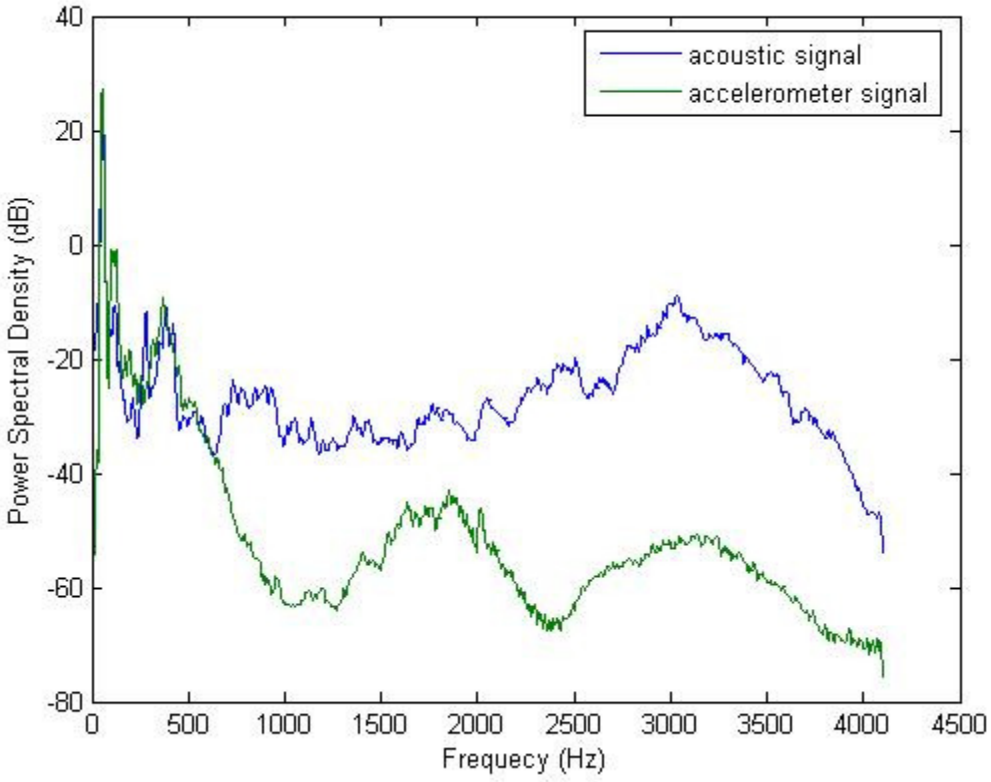

Figure 4.5: PSD levels for the accelerometer and rear-facing microphone (0 to 4096 Hz).

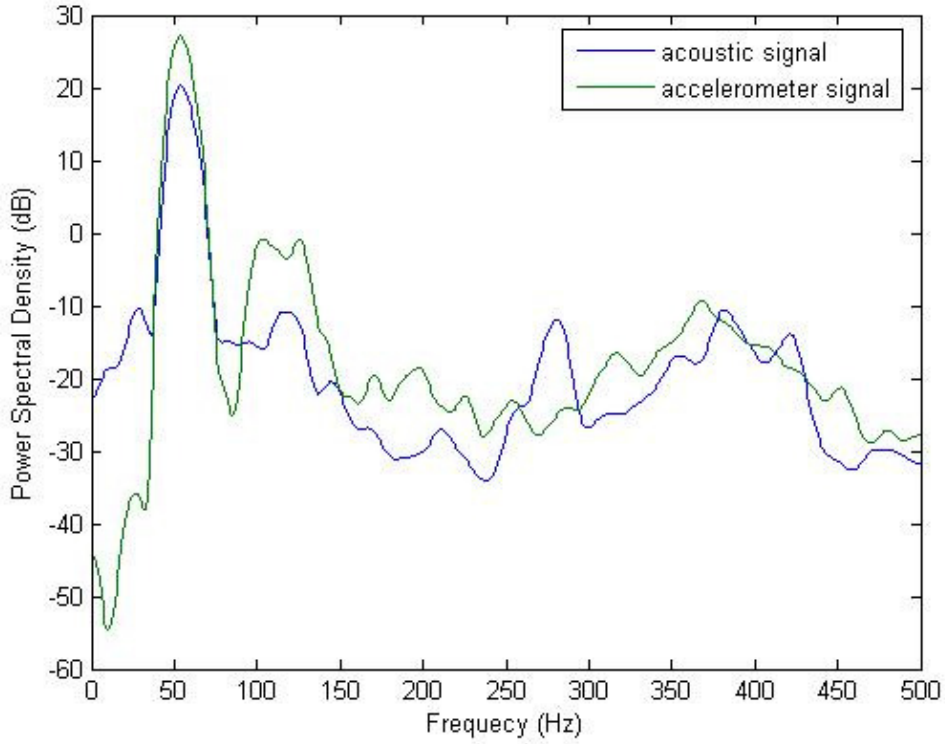

Figure 4.6: PSD levels for the accelerometer and rear-facing microphone (0 to 500 Hz).

The accelerometer and the microphone pick up similar frequency components in the 0 to 500 Hz range. This indicates that the accelerometer signal may represent the low-frequency sound produced by the engine and picked up by the microphone. Further experimentation with the LMS filtering algorithm is warranted by this relationship.

There are several variables in a practical LMS algorithm that must be adjusted. Among these are the length of the FIR filter and the convergence factor. The convergence factor determines how quickly each successive coefficient of the filter converges to the optimal solution. For this implementation of the algorithm, the convergence factor can be any value between zero and one. After some trial and error, it was found that using the LMS algorithm with a filter length of 1/16 of the sampling frequency and a convergence coefficient of 0.8 produced a noticeable reduction of the engine noise. Figure 4.7 shows the difference in the amplitudes of each signal, which is not notable in itself. However, Figure 4.8 shows that this reduction in noise level occurred entirely within the low frequency range where the engine produces most of its energy.

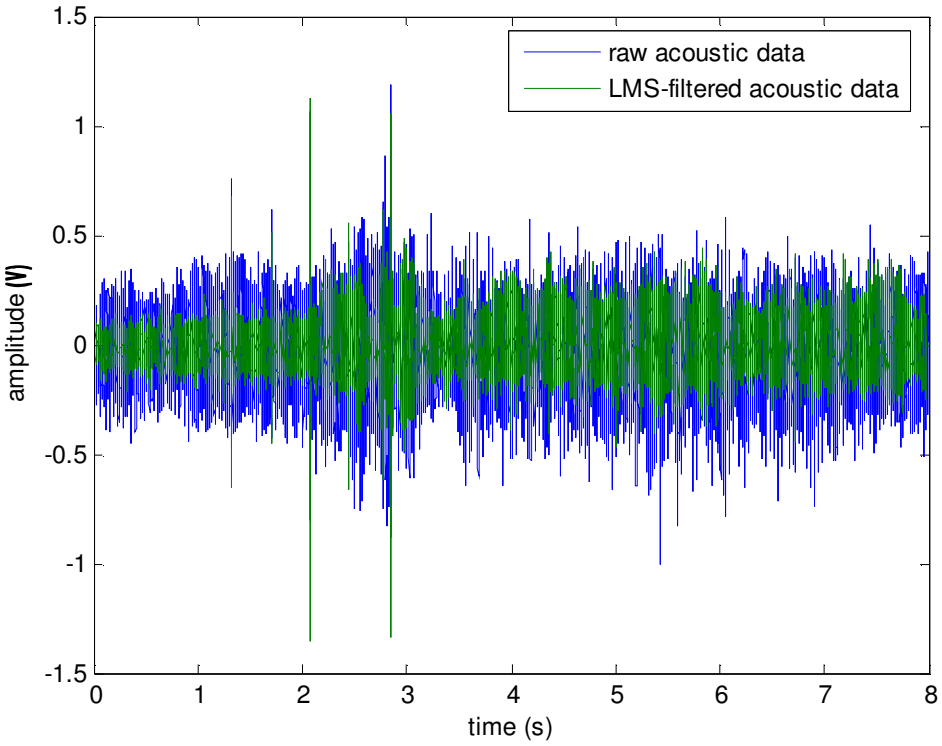

Figure 4.7: Comparison of raw acoustic data and with LMS-filtered data.

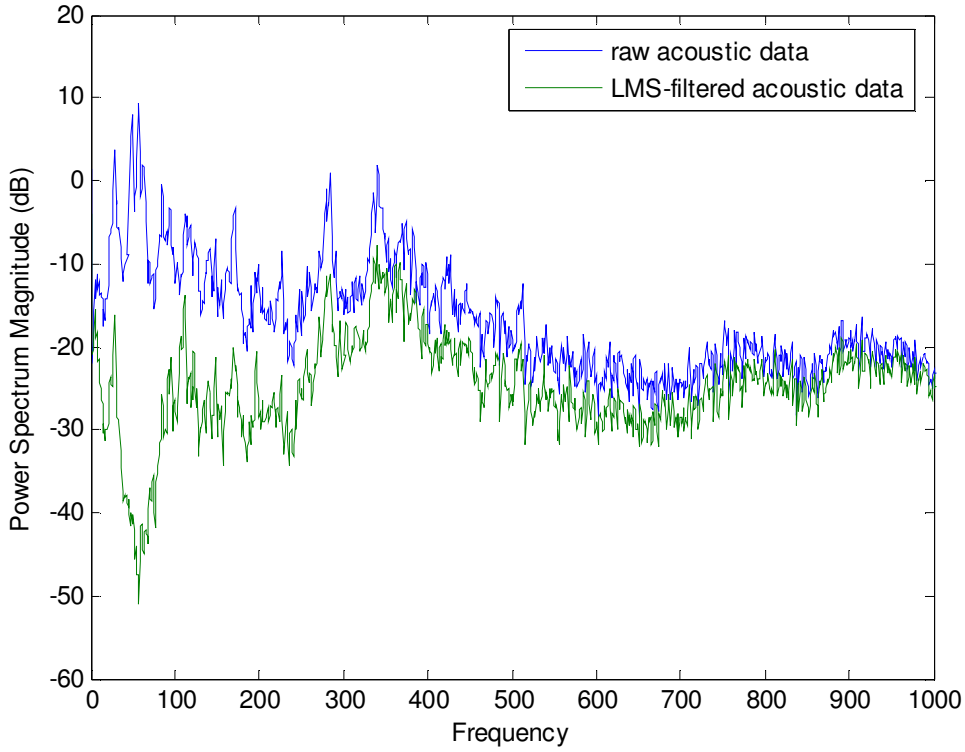

Figure 4.8: Comparison of power spectral densities of raw acoustic data and LMS-filtered acoustic data.

To further evaluate the effectiveness of the LMS algorithm for this application, it is useful to use a metric called impulsiveness that is used by the "Node Processer" code to select impulsive acoustic events. Dan Mennitt defines impulsiveness as

$$imp(k) = \frac{|r(k)|}{\text{median}(|r|)} \tag{4.1}$$

where *r(k)* is an acoustic signal and *k* is the sample number of the impulse to be evaluated [2]. According to Equation 4.1, the maximum impulsiveness of the signal improved from 10.2 before the LMS-filtering to 30.6 after filtering. This improvement in impulsiveness can be seen in Figure 4.9. In practice, this algorithm could be used to reduce the effect of the engine noise on the Node Processor program and allow for detection of fainter sources during engine operation.

However, the LMS-filtering algorithm was not successfully implemented with the Node Processer code as it is beyond the scope of this project. This demonstration does

demonstrate that an accelerometer can be used to reduce the effect of engine noise on a mobile acoustic sensor node.

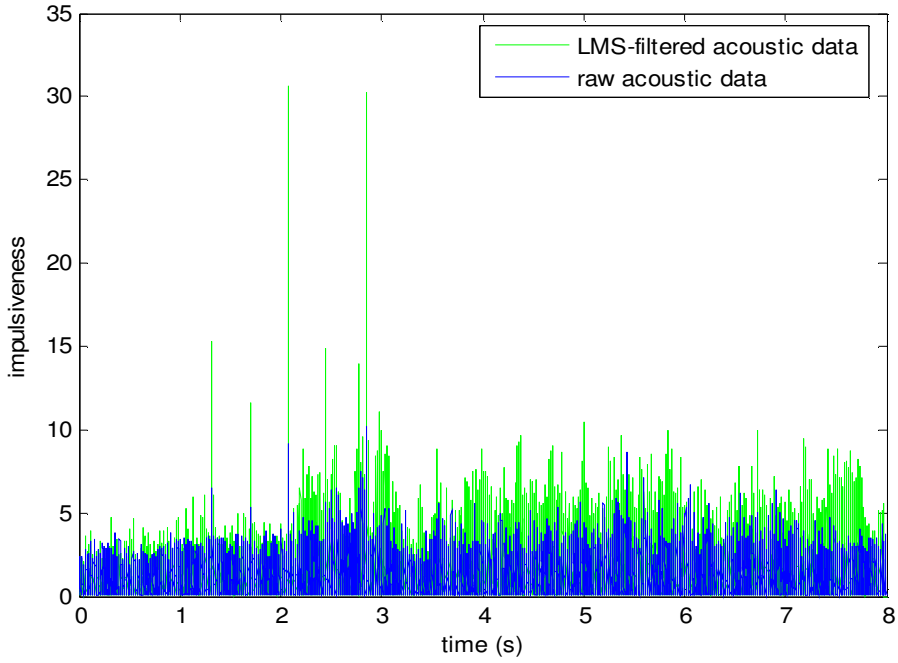

Figure 4.9: Impulsiveness of raw acoustic signal and LMS-filtered acoustic signal.

Chapter 5: Demonstration of Performance

5.1 Camera Tracking by Acoustic Localization

An experiment was conducted to demonstrate that the camera can record images of an acoustic source tracked by the acoustic node. The experiment was conducted in the laboratory space of VAL. The front equipment rack of the ATV was removed from the ATV and placed on blocks on top of table. The camera was about 1.5 m off the ground, with the camera's neutral position facing an open area. The camera, camera servo controller, and the acoustic node were all connected to a laptop to control the motion of the camera and record the resulting video. Modified "Node Processor" code processed the acoustic data and controlled the camera servo. The code directed the camera servo to aim the camera at the azimuth bearing angle of the source. A video capture program, "AMCAP", was used to record a video file of the camera view. The tester held a speaker

approximately 1.5 meters above the ground and walked in an arc approximately two meters away from the node while the speaker played a constant 200 Hz tone.

Throughout the test sequence, several passes were made across the total range of the camera. Figure 5.1 shows several screenshots extracted from the video of the speaker making one pass around the room.

Figure 5.1: Screenshots of camera tracking test in VAL lab.

Ideally, the speaker would remain in or very close to the center of every image. Because of inaccuracy of acoustic localization and delays in the servo control of camera movement, the image jumps around while tending to lag behind the true position of the speaker. However, throughout the entire testing sequence, the camera only lost track of the speaker a few times, and during many trials, the camera maintained a constant image of the speaker and tester. This test effectively demonstrates the concept of sensor integration, as a target was tracked visually using only audio input.

5.2 ATV Performance as a Mobile Sensor Platform

The main tests for determining the effectiveness of a mobile sensor platform were conducted at Virginia Tech's Kentland Farms facility outside of Blacksburg, VA between October 30th and November 1st, 2007. There were multiple configurations testing the performance of the acoustic localization and sensor fusion software as well as the ATV sensor platform. This section will focus on the tests that evaluated the ATV's performance as a solitary mobile acoustic sensor.

In order to test the effectiveness of the sensor platform, the ATV took a planned path through the test area while a stationary acoustic source produced either tonal or impulsive sound. The tonal source was a loudspeaker playing an intermittent 200 Hz tone. The speaker played the tone for ten seconds then no sound for ten seconds before repeating. The impulsive source was a cap gun that was fired once every ten to twenty seconds.

Many tests were conducted but due to the difficulties of outdoor testing only one/a few gave useful data. This section will show the results of a test conducted during the afternoon of November 1st. The ATV followed a path in the vicinity of the source and stopped at three points, turning off the engine to listen for sources. Figure 5.2 shows the path of the ATV and the three locations where the ATV was stopped in order to better detect the acoustic source.

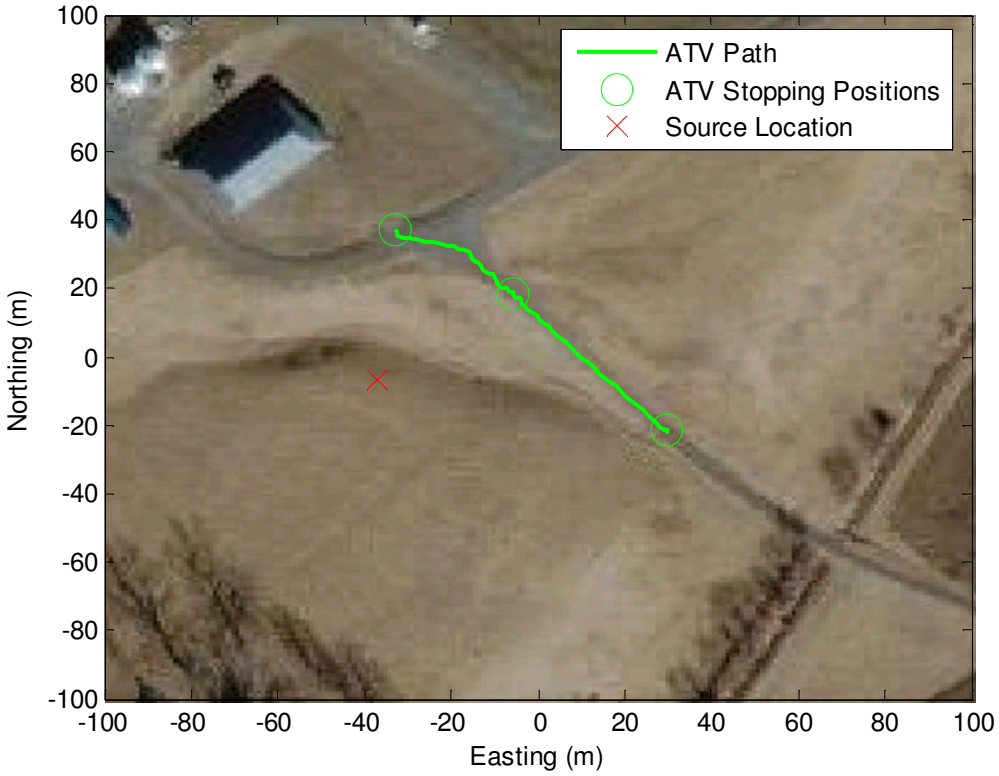

Figure 5.2: ATV Path, ATV Stopping Locations and Source Location.

For this test, the tonal source was placed on a hill overlooking a gravel road that connected the test area with lower fields in the area. The ATV traveled down this gravel road for the entirety of the test.

The test lasted three minutes. The Node Processor software detected many tonal sources as well as impulsive sources. For the purposes of this analysis, detections recorded while the ATV's engine was moving were eliminated in post-processing due to a large number of irrelevant detections. The ATV's acoustic node most likely picked up the engine noise and noise of the tires rolling on gravel. While the ATV was stopped and the engine turned off, the software detected the tone during thirty separate seconds of the test. Figure 5.3 shows a map of all of these detections.

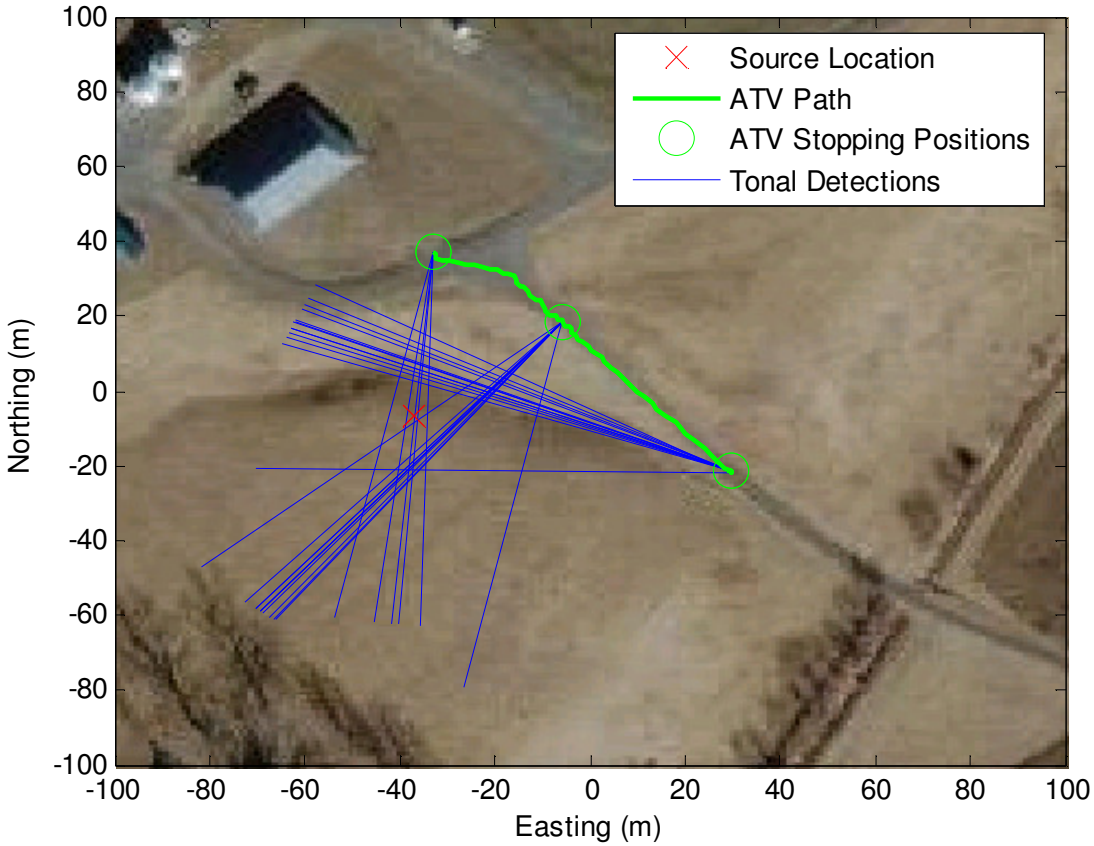

Figure 5.3: Acoustic detections while ATV was stopped.

The acoustic node detected the general direction of the source in all three locations. However, there was significant variance in the detection angle at each location. For the purposes of estimation, the detections at each location were averaged and plotted. This plot is shown in Figure 5.4.

Figure 5.4: Averaged detection angles for all three positions.

Figure 5.4 shows how the real time detections combined with some post-processing can estimate the location of the acoustic source. For the purposes of this paper, the estimated location is the average of the three vertices of the triangle formed by the three bearing estimations. The estimation error, or distance between the actual and estimated source location, is 4.65 meters. This error is likely a combination of errors from several aspects of the system, including the microphone array, the acoustic localization algorithm, the electronic compass and the GPS receiver.

There are several other ways to estimate the position of a source from three azimuth angle estimations. These will not be covered in this paper, but these methods have been explored for this application in Dan Mennitt's doctoral thesis [2].

Chapter 6: Conclusions and Future Work

The goal of this project was to construct a mobile sensor platform to demonstrate the effectiveness and feasibility of such a platform for field use. The ideal platform would be semi-autonomous, i.e. capable of operation with limited human input, as well as able to transmit audio and video data simultaneously. This platform did not have these capabilities, but it did successfully demonstrate several aspects of a mobile sensor platform as a standalone unit or as a node in a larger detection network.

First, the system showed effective visual tracking of a target using only audio information. The camera tracking experiment initially confirmed what other work had already proven, that the microphone array coupled with the Node Processor software can track a target emitting noise [1]. However, the experiment also demonstrated that the output from the already proven tracking algorithm can be used to obtain images of a moving target in near-real-time. This feature would be especially useful in a combat environment, where real-time images of a sniper or moving vehicle would be essential for indentifying targets and maintaining situational awareness.

Next, and more importantly, the system showed that a mobile node can triangulate the position of a stationary target over a relatively short amount of time and that a network of such mobile nodes can triangulate the position of a target nearly instantly. In a field test, the ATV moved to three different locations to listen for the presence of an acoustic source. The acoustic localization algorithm obtained several detections of the source at each location. It was shown that once these detections were averaged, the system detected the direction of the source with little error. It is important to note that all of the localization vectors shown in this paper were transmitted to a central fusion center in real time. If instead of one mobile sensor node at three locations, there were three identical sensor nodes at those locations, the same result could have been obtained in a matter of seconds. This has been demonstrated more thoroughly in Dan Mennitt's work [2]. This paper also showed that localization of acoustic sources with large interfering engine noise is plausible, although this was not successfully demonstrated in the field.

The feasibility of acoustic source localization with one mobile node was only able to be demonstrated in a single test by the successful combination of all parts of the

system. The outfitting of the ATV for remote operation allowed the test to be conducted in real time with a single node as the ATV was able to move from position to position, stopping, cut off the engine, listening, restarting and relocating with no direct human manipulation. The GPS antenna and electronic compass allowed the system to record its own position and orientation. Finally, the embedded computer and wireless antenna allowed the system to decode the acoustic data and transmit detection information as well as the information of the node's position and orientation to a separate fusion center. This replicates the real-world operation of such a system in that the information gathered by the system could be viewed and processed in a fairly safe location removed from the urban combat environment.

In order to further demonstrate the effectiveness of such a system, several features would have to be added to the mobile sensor node. First, not all useful elements of the system were successfully operated in the field at the same time. Ideally, the mobile node would be able to send images captured by the onboard camera to the fusion center via wireless network. Due to several technical issues this was not possible under this project. Foremost among these issues was the difficulty in sending a large piece of data like an image without interrupting the collection of acoustic information. Also, while the LMS filtering algorithm proved to be effective in reducing engine noise in some test cases, it was never demonstrated in a field environment along with the acoustic localization algorithm. If properly implemented at the time, the LMS filtering algorithm may have allowed for localization of acoustic sources while the ATV engine is running. A real-world version of this system should be able to operate either autonomously or in a "semi-autonomous" mode. In a semi-autonomous mode, the mobile node would move based on general inputs received over the wireless adapter, such as "move to location (x,y)" or "move 10 meters forward". Either of these modes would require all actuators to respond from inputs from the embedded computer, as well as the addition of a velocity-feedback component. Finally, this system should be demonstrated in a true urban environment. The field testing was performed in an environment with hills as obstacles and moderately close building to create multipath effects, but it did not have the density or size of buildings that would be present in an urban environment. To truly investigate and overcome the effects of multipath and obstruction, testing in a replicated urban

environment would need to be pursued. All of these additions are feasible and may be continued in future projects.

Bibliography

[1] Gillett, P. W. Head Mounted Microphone Arrays. Dissertation. Virginia Polytechnic Institute and State University, 2009.

[2] Mennitt, D. J. Multiarray Passive Acoustic Localization and Tracking. Dissertation. Virginia Polytechnic Institute and State University, 2009.

[3] Simon, G., et al. "Sensor Network-Based Countersniper System," Proc. of the 2nd International Conference on Embedded Networked Sensor Systems, pp. 1-12, Nov 3-5, 2004.

[4] Hengy, S. "Sniper Localization Using a Helmet Array," In Battlefield Acoustic Sensing for ISR Applications (pp. 7-1 – 7-16). Meeting Proceedings RTO-MP-SET-107, Paper 7. Neuilly-sur-Seine, France: RTO, 2006.

[5] Hengy S., Demezzo, S. and Hamery, P. "Sniper Detection Using a Helmet Array: First Tests in Urban Environment," Proc. of SPIE Vol. 6562 (2007).

[6] Young, S. H. and Scanlon, M. V. "Robotic Vehicle Uses Acoustic Array for Detection and Localization in Urban Environments," Proc. SPIE, Vol. 4364, 264 (2001).

[7] Young, S. H. and Scanlon, M. V. "Detection and Localization with an Acoustic Array on a Small Robotic Platform in Urban Environments," Technical Report ARLTR-2575, Army Research Laboratory, Adelphi, MD, January 2003.

[8] Martin, P. J. and Young, S. H. "Collaborative Robot Sniper Detection Demonstration in an Urban Environment," Proc. SPIE, Vol. 5422, 271 (2004).

[9] "The Bug – Precision Linear Actuator from Ultra Motion." Ultramotion. Nov. 1, 2006. < http://www.ultramotion.com/products/bug.php>

[10] "4" Stroke 200 lbs Force Linear Actuator." Firgelli Automations. Nov. 1, 2006. <http://www.firgelliauto.com/product_info.php?cPath=79&products_id =95>

[11] "HS-5995TG High Speed Metal Gear Servo." Hitec RCD. Nov. 6, 2006. <http://www.hitecrcd.com/products/servos/digital/digital-sport/hs-5995tg.html>

[12] "Optic 6 - 2.4GHz." Hitec RCD. Nov. 6, 2006. <http://www.hitecrcd.com/products/transmitters/aircraft/optic-6-2-4ghz.html>

[13] “Supreme 7 - 7 Channel 2.4GHz Receiver.” Hitec RCD. Nov. 6, 2006. <http://www.hitecrcd.com/products/receivers/aircraft/2-4ghz/supreme-7.htm>

[14] “Motion Mind (Hardware Version 2 Only) Motor Controller Data Sheet.” Solutions-Cubed.com. Nov. 9, 2006. <http://www.solutions-cubed.com/solutions%20cubed/Products%20Page/Downloads/MOTMDS_10.pdf>

[15] Hambley, A. R. Electrical Engineering: Principles and Applications. Prentice Hall, Upper Saddle River, New Jersey, 2002, Chs. 4, 13.

[16] “Relio R1220, 1GHz ULV Celeron M, 512MB RAM (R1220).” Sealevel Systems. Nov 18, 2006. <http://www.sealevel.com/product_techspecs.asp?product_id=1135&Industrial%5FComputer%2C%5FRackmount%2C%5FPC%2C%5FXPe%2C%5FXP%5Fembedded>

[17] Inman, D.J. Vibration with Control. Wiley, West Sussex, England, 2006, Ch. 6.

[18] “DT9816 Low Cost USB DAQ Module.” Data Translation. Nov. 13, 2006. <http://www.datatranslation.com/products/dataacquisition/usb/dt9816.asp>

[19] Solo, V., and X. Kong, 1995. Adaptive Signal Processing Algorithms. Prentice-Hall, Englewood Cliffs, New Jersey, 1995.

[20] “TCM Legacy : Digital Compass Modules.” PNI Sensor Corporation. Jan 2007. <http://www.pnicorp.com/products/all/tcm-legacy>